Catalytic and electrochemical exploitation of polyoxometalates

Outline

- Introduction to polyoxometalates (POMs)
- Exploitation of POMs for catalytic processes
- Synthesis of bio-degradable polymer, Poly lactic acid (PLA)
- Synthesis of Methoxy methyl chloride (MOM-Cl)
- Exploitation of POMs for the synthesis of carbon supported metal nanoparticles
- POMs as redox switch - metal nanoparticle- conducting polymer - nanocomposites
- Application of POM stabilized carbon supported metal nanoparticles
- Ru/STA-C for electrochemical supercapcitor applications
- Pt/STA-C and Pt-Ru/STA-C for electrocatalytic metahanol oxdation reaction
- Pt/STA-C for oxygen reduction reaction

Preparation of POM stabilized metal nanoparticles

Synthesis of metal nanoparticles

- Reduction of metal salts
  - Alcohol reduction
  - Borohydride reduction
  - Citrate reduction
  - Polyol process
- Photolytic reduction
- Thermal decomposition
- Electrolysis of bulk metals

Often needs stabilizing agent to prevent agglomeration

Advantages of reduced POMs as suitable reducing agents for the synthesis of metal nanoparticles

- Redox potentials can be tuned finely to match that of many metal ions

Reduction of POMs

- Photochemically
- Through ^{60}Co γ-radiolysis
- Electrolytically
- With reducing reagents

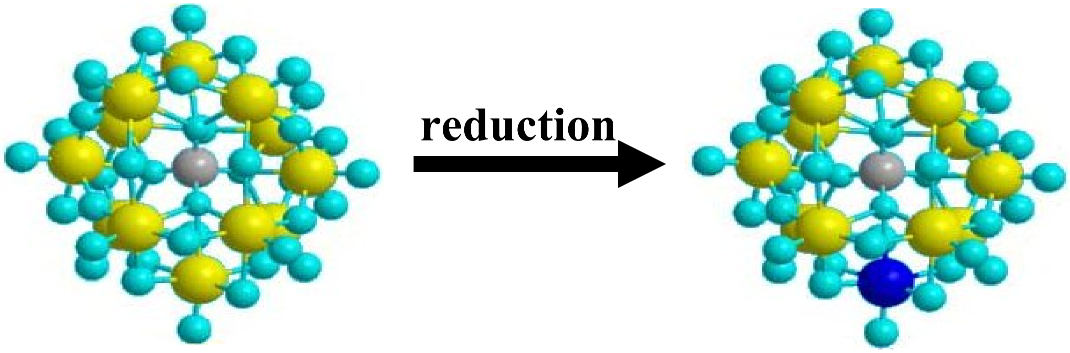

$H_4SiW_{12}O_{40}^{4-}$ $H_4SiW_{12}O_{40}^{5-}$

- The reduced and oxidized forms are stable in a large pH domain
- Transfer electrons efficiently
- POMs are insensitive to dioxygen – No storage problems
- Stabilizes the nanoparticles efficiently
- Adsorbs strongly on the metal nanoparticles

Potential scale for polyoxometalates and metals

Redox potentials of various POMs

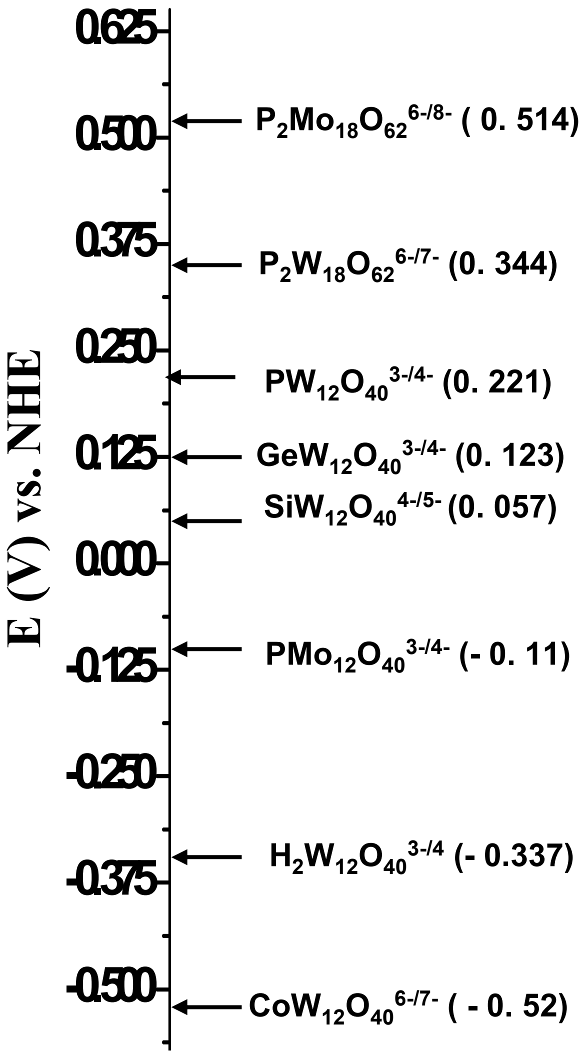

$P_2Mo_{18}O_{62}^{6-/8-}$ (0. 514)

$P_2W_{18}O_{62}^{6-/7-}$ (0. 344)

$PW_{12}O_{40}^{3-/4-}$ (0. 221)

$GeW_{12}O_{40}^{3-/4-}$ (0. 123)

$SiW_{12}O_{40}^{4-/5-}$ (0. 057)

$PMo_{12}O_{40}^{3-/4-}$ (- 0. 11)

$H_2W_{12}O_{40}^{3-/4}$ (- 0.337)

$CoW_{12}O_{40}^{6-/7-}$ (- 0. 52)

Redox potentials of various Metals

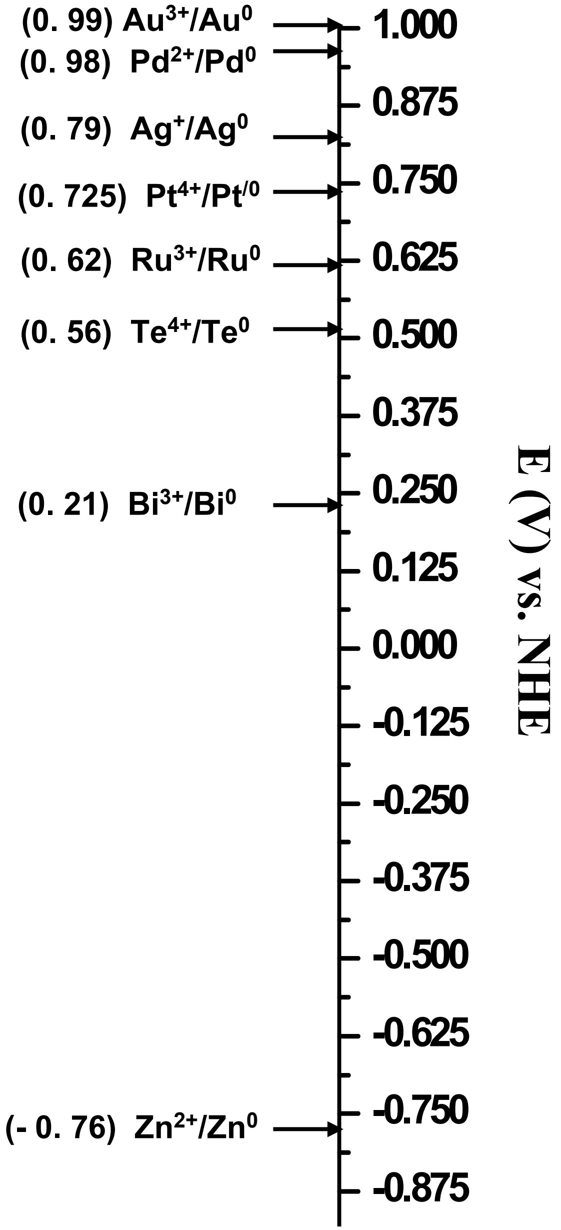

(0. 99) Au^{3+}/Au^0

(0. 98) Pd^{2+}/Pd^0

(0. 79) Ag^+/Ag^0

(0. 725) $Pt^{4+}/Pt^{/0}$

(0. 62) Ru^{3+}/Ru^0

(0. 56) Te^{4+}/Te^0

(0. 21) Bi^{3+}/Bi^0

(- 0. 76) Zn^{2+}/Zn^0

Formation of colloidal carbon nanoparticles using POM

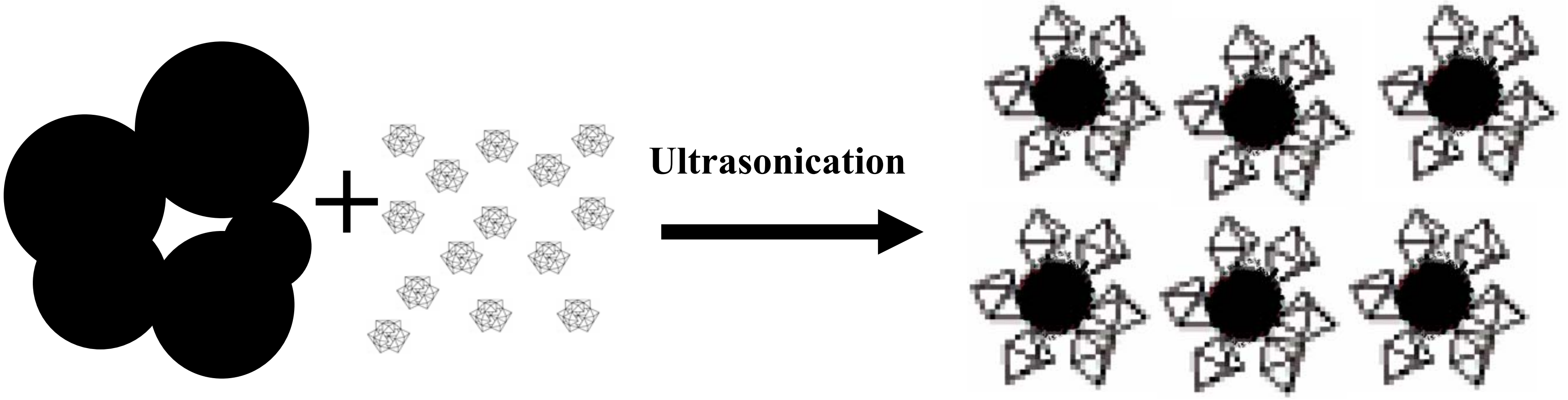

Carbon

$H_3PMo_{12}O_{40}$ Solution

Ultrasonication

Carbon nanoparticles stabilized by POM

TEM Image

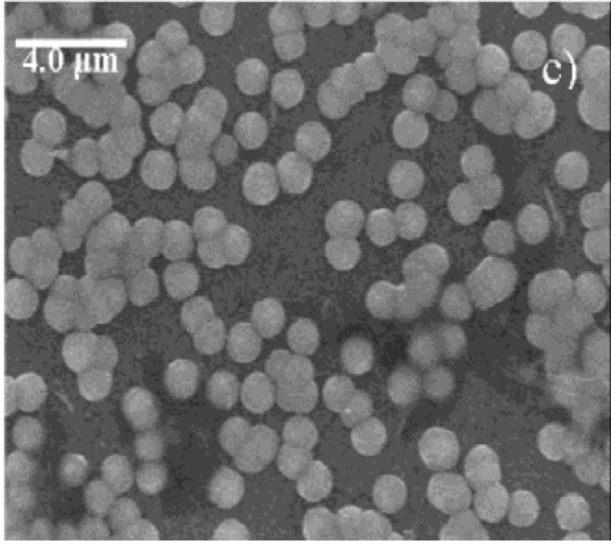

SEM image

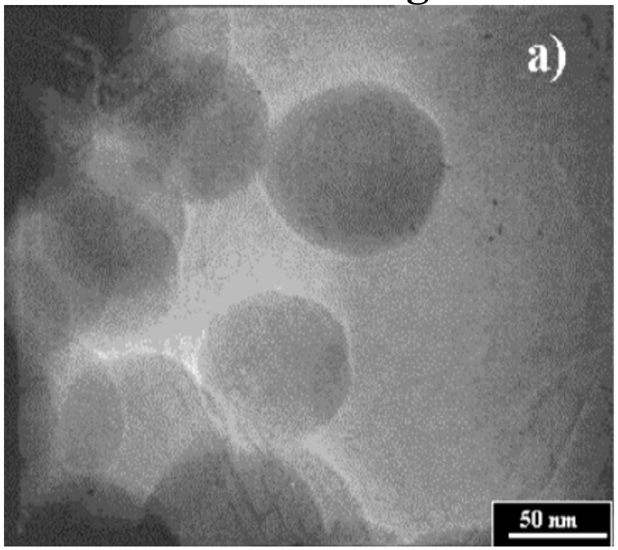

Chemistry of Materials, 16, 2004, 2984-2986

Controlled synthesis of CNTs using POM

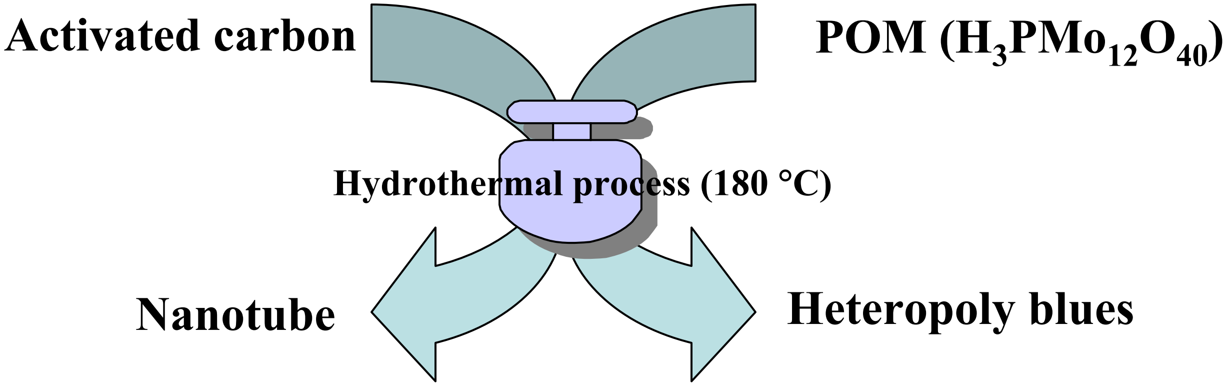

Activated carbon

POM ($H_3PMo_{12}O_{40}$)

Hydrothermal process (180 °C)

Nanotube

Heteropoly blues

TEM images (a and b) of CNTs and HRTEM image of the CNTs

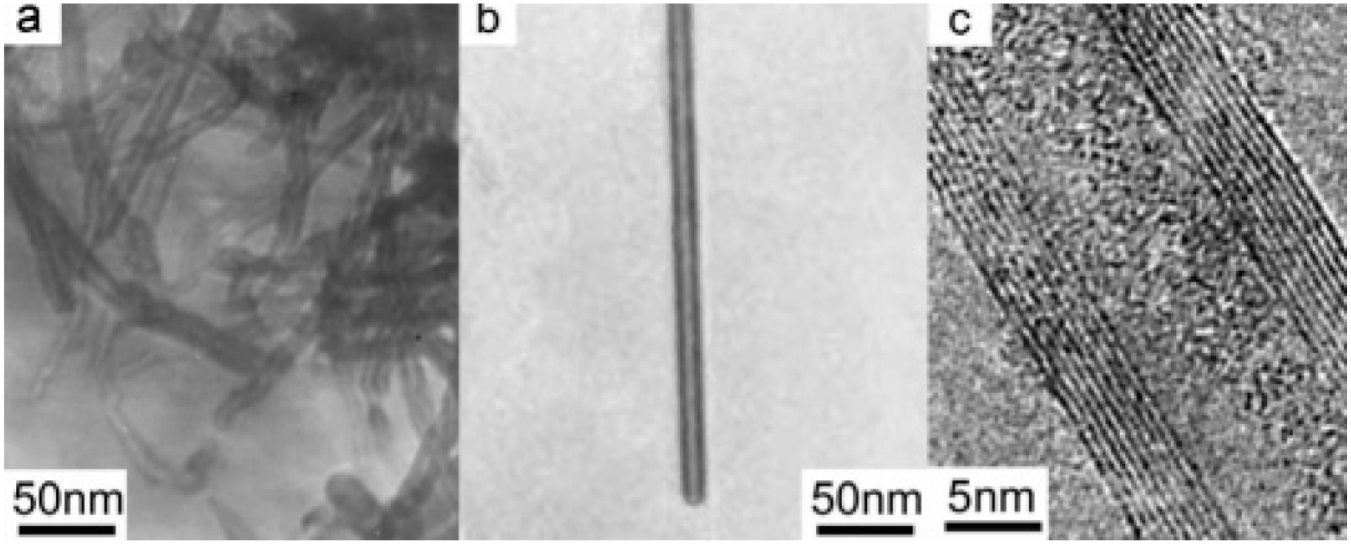

Journal of American Chemical Society, 127, 2005, 6534-6535

Synthesis of metal nanoparticles supported on carbon nanostructures using POMs

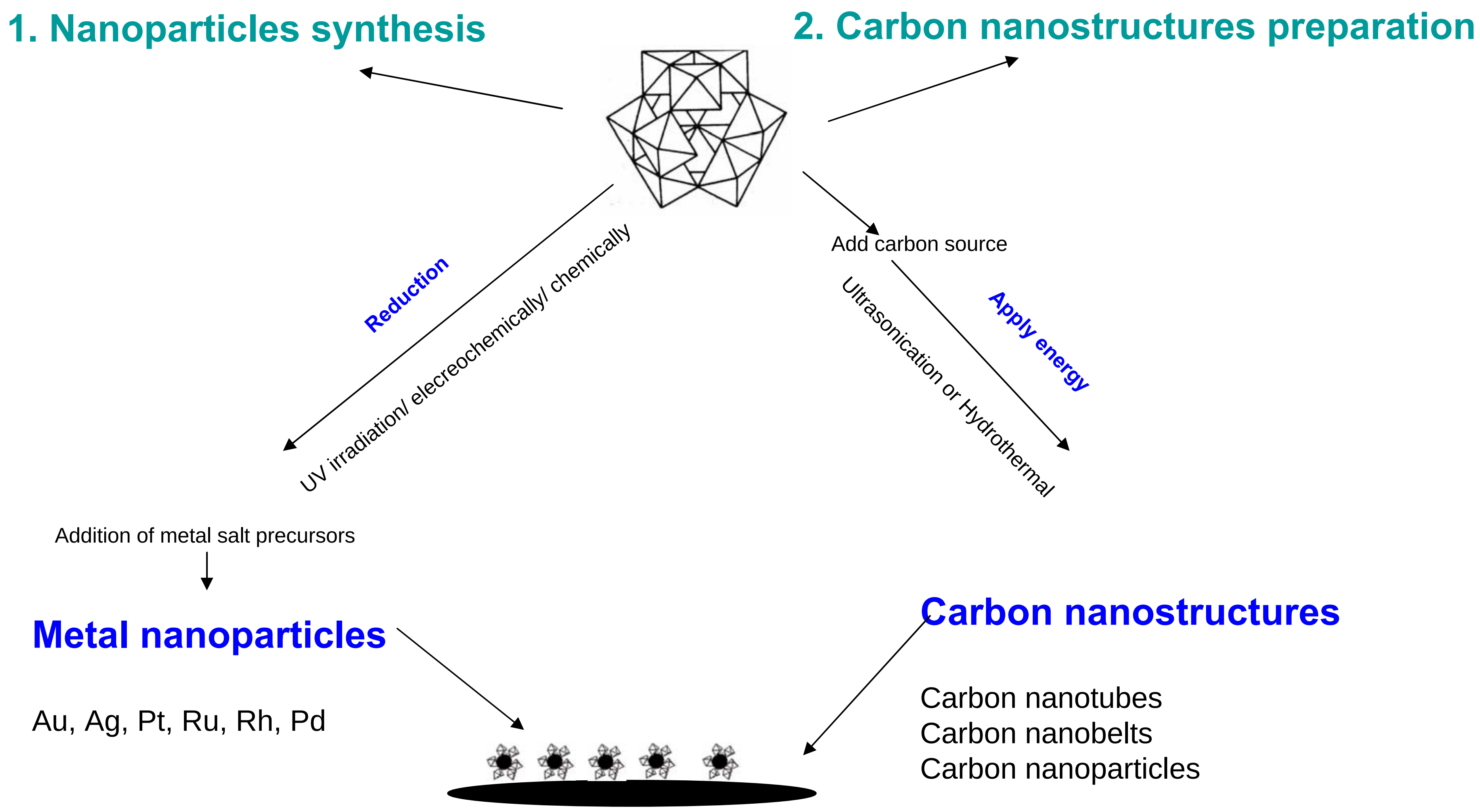

1. Nanoparticles synthesis

2. Carbon nanostructures preparation

Reduction

UV irradiation/ elecreochemically/ chemically

Addition of metal salt precursors

Metal nanoparticles

Au, Ag, Pt, Ru, Rh, Pd

Add carbon source

Apply energy

Ultrasonication or Hydrothermal

Carbon nanostructures

Carbon nanotubes
Carbon nanobelts
Carbon nanoparticles

Synthesis of Pt nanoparticles stabilized by POMs

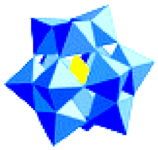

$SiW_{12} + Zn \longrightarrow \text{Reduced } SiW_{12}$

(Colourless) (blue)

Molar ratio
(1 : 10)

10mM $H_4SiW_{12}O_{40}$
(4 mL) in H_2O

Zn metal powder

Add

Remove excess zinc by filtration

Reduced SiW_{12}(STA)

$\text{Reduced } SiW_{12} + Pt^{4+} \longrightarrow Pt^{0}\text{- oxidized } SiW_{12}$

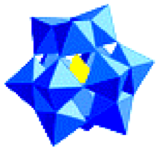

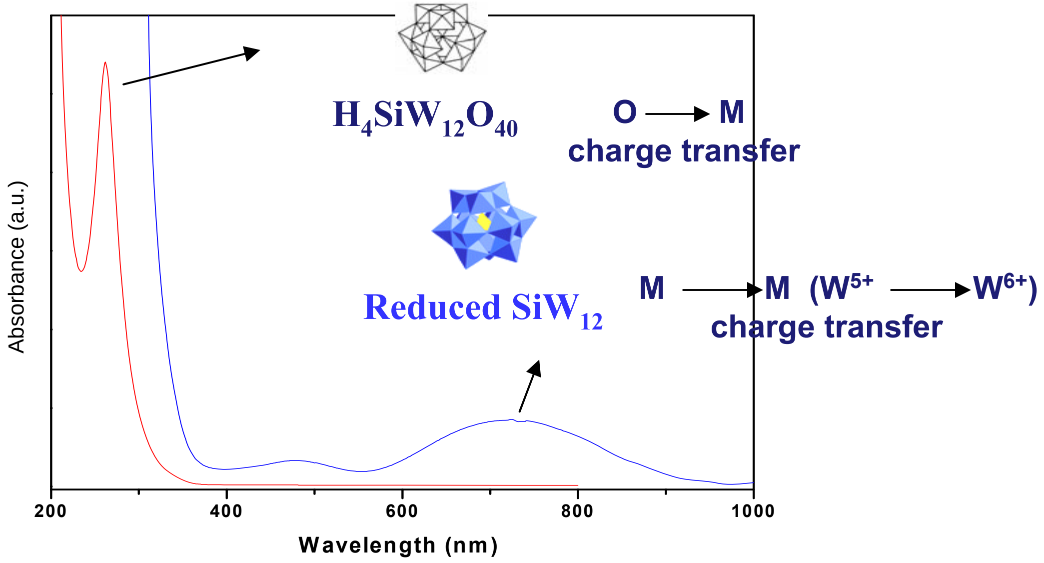

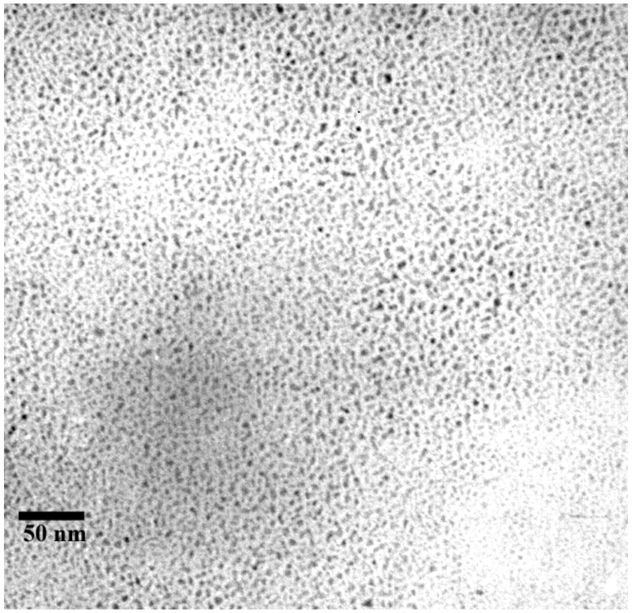

TEM image

Synthesis of Pt nanoparticles supported on carbon using POMs

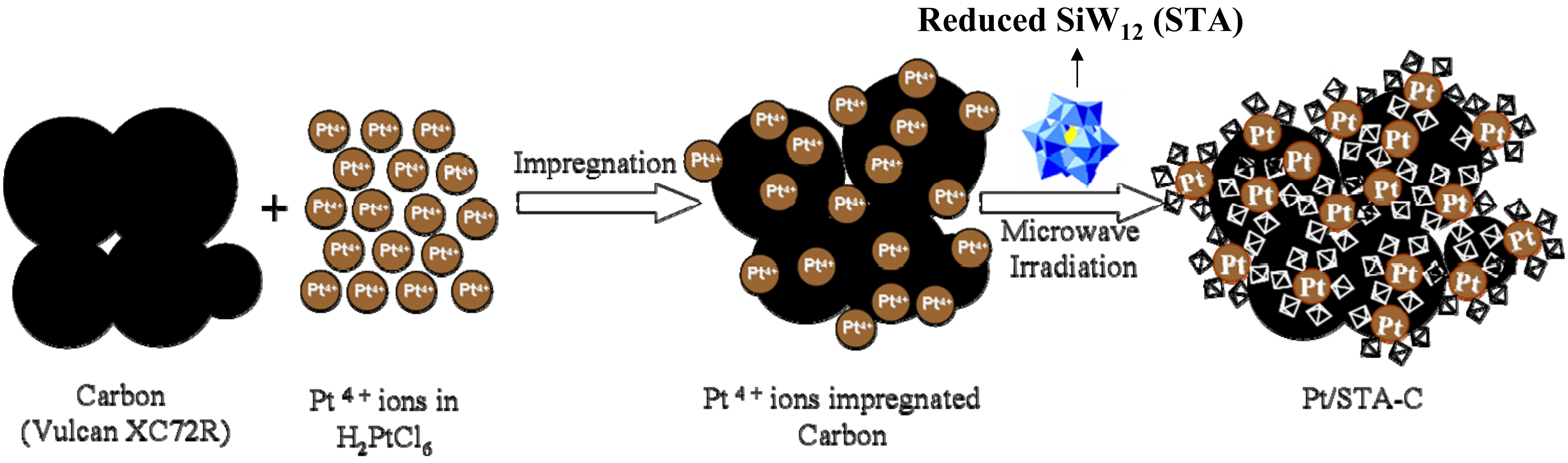

The strategy has been extended for the synthesis of

- 20% Pt-Ru/STA-C
- 20% Ru/STA-C
- 20% Pd/STA-C

Synthesis of 20% Pt/STA-C

10mM H_2PtCl_6

20 mg Vulcan XC72

Stirred for 3 h

Evaporated to dryness

Add 4mL of Reduced STA

Microwave irradiation for 30 sec

Washed with H_20 & centrifuged

Dried

20% Pt/STA-C

Using the above strategy
20% Pt-Ru/STA-C, 20% Ru/STA-C, 20% Pd/STA-C, 20% were prepared

TEM Analysis and Particle size distributions of 20% Pt/STA-C and 20% Pt-Ru/STA-C

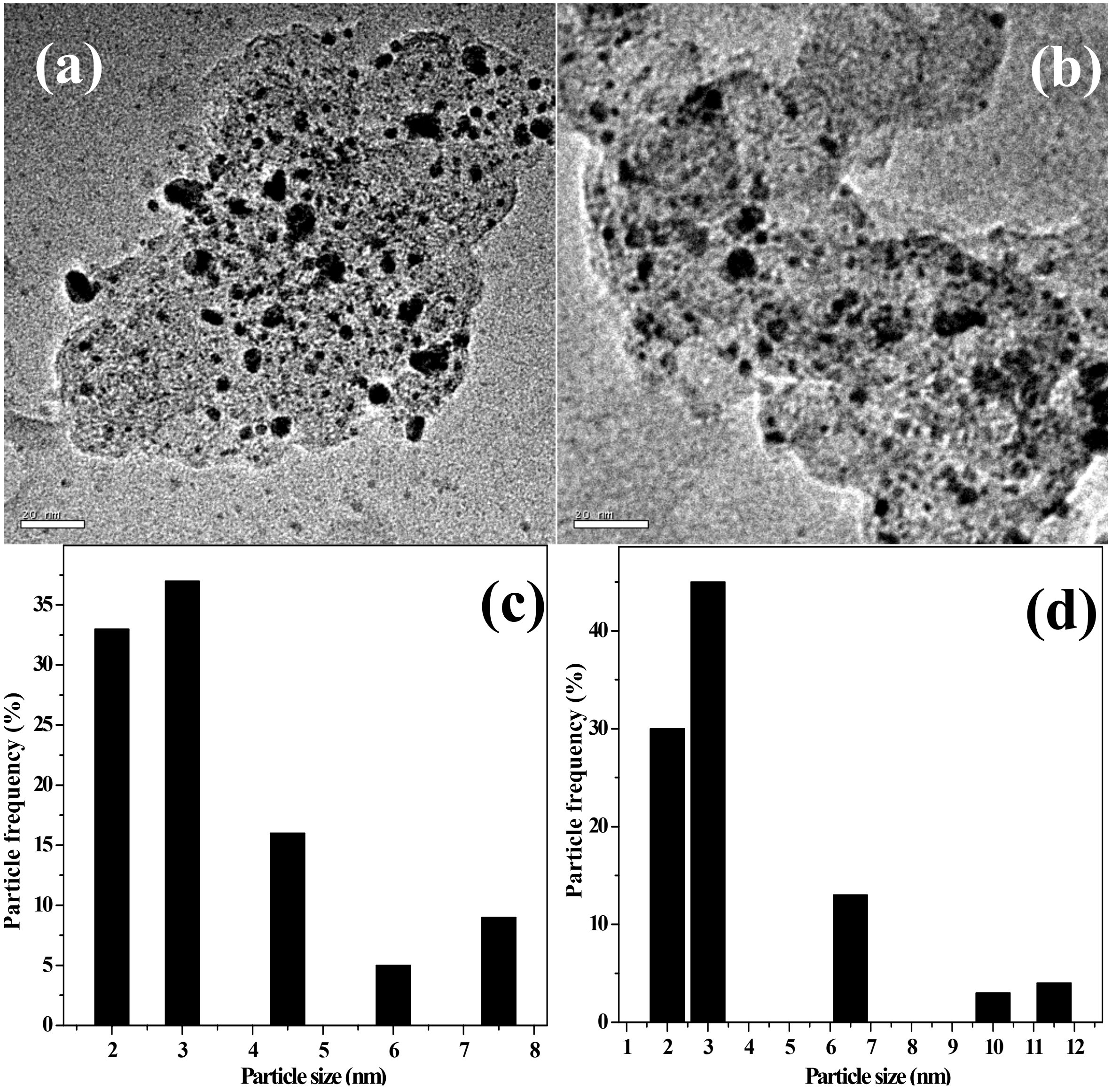

- (a) Pt/STA-C
- (b) PtRu/STA-C
- (c) Particle size distribution from (a)
- (d) Particle size distribution from (b)

HRTEM and EDX Analysis of Pt/STA-C and Pt-Ru/STA-C

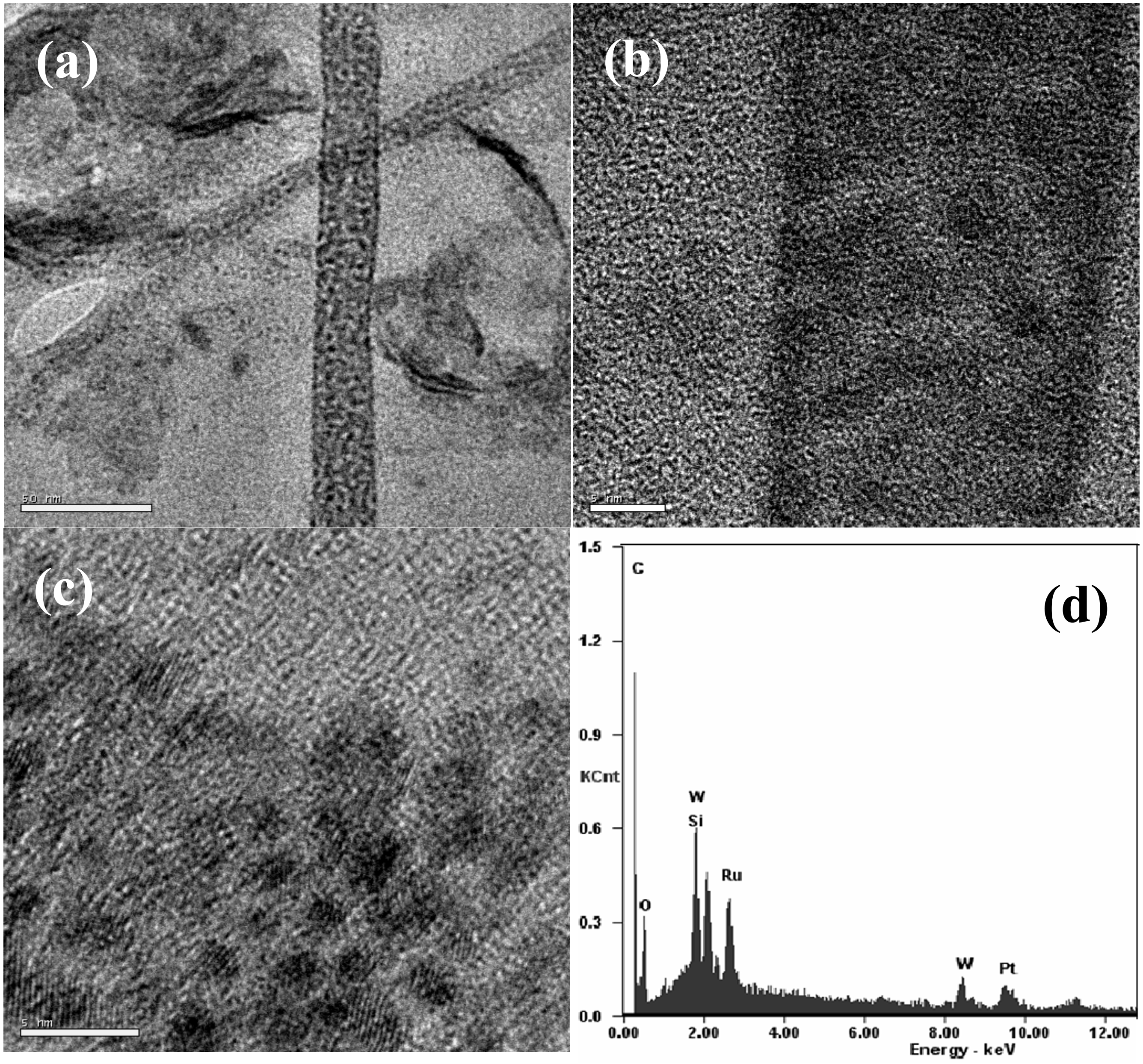

(a) & (b) HRTEM of Pt/STA-C

(c) HRTEM of Pt-Ru/STA-C

(d) EDX of Pt-Ru/STA-C

TEM and HRTEM Images of 20% Pd/STA-C

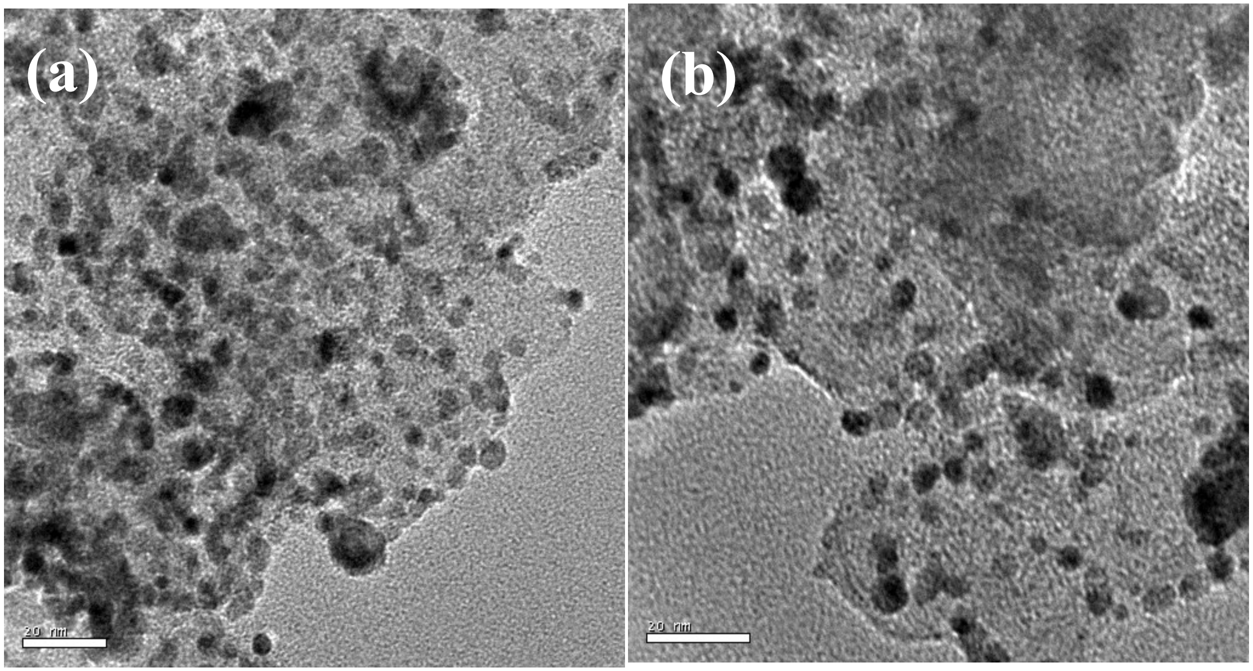

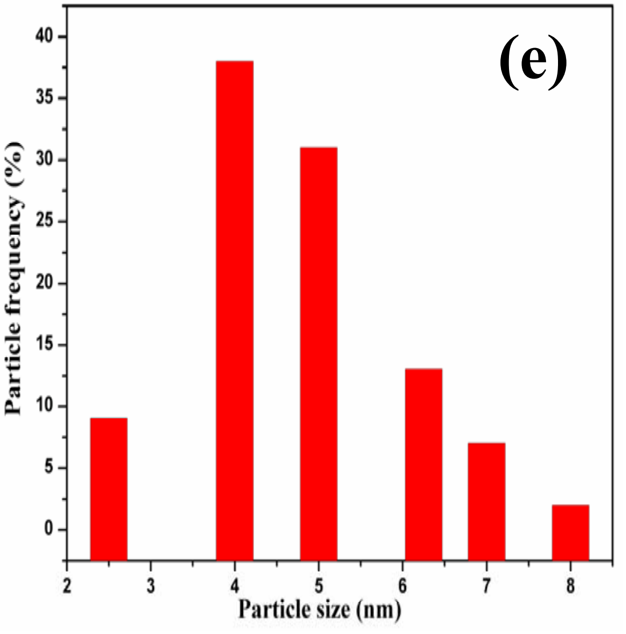

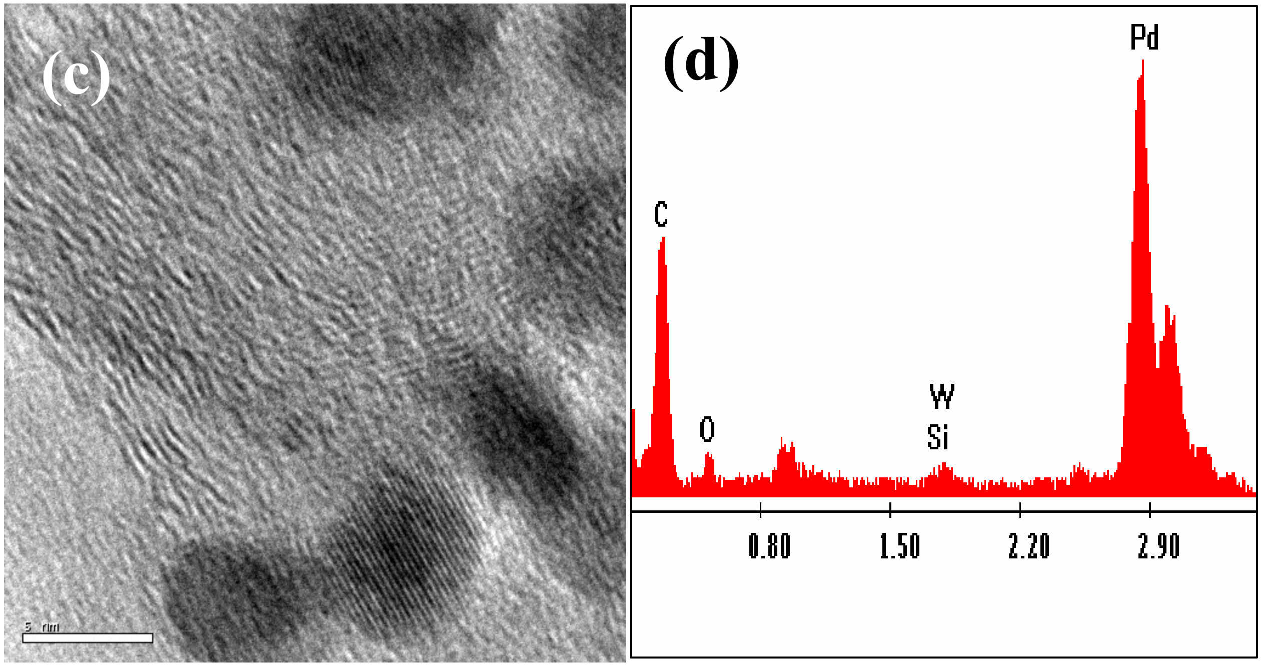

(a) & (b) TEM of Pd/STA-C

(c) & (d) HRTEM of Pd/STA-C

(e) Particle size distribution of Pd/STA-C

TEM and HRTEM Images of 20% Ru/STA-C

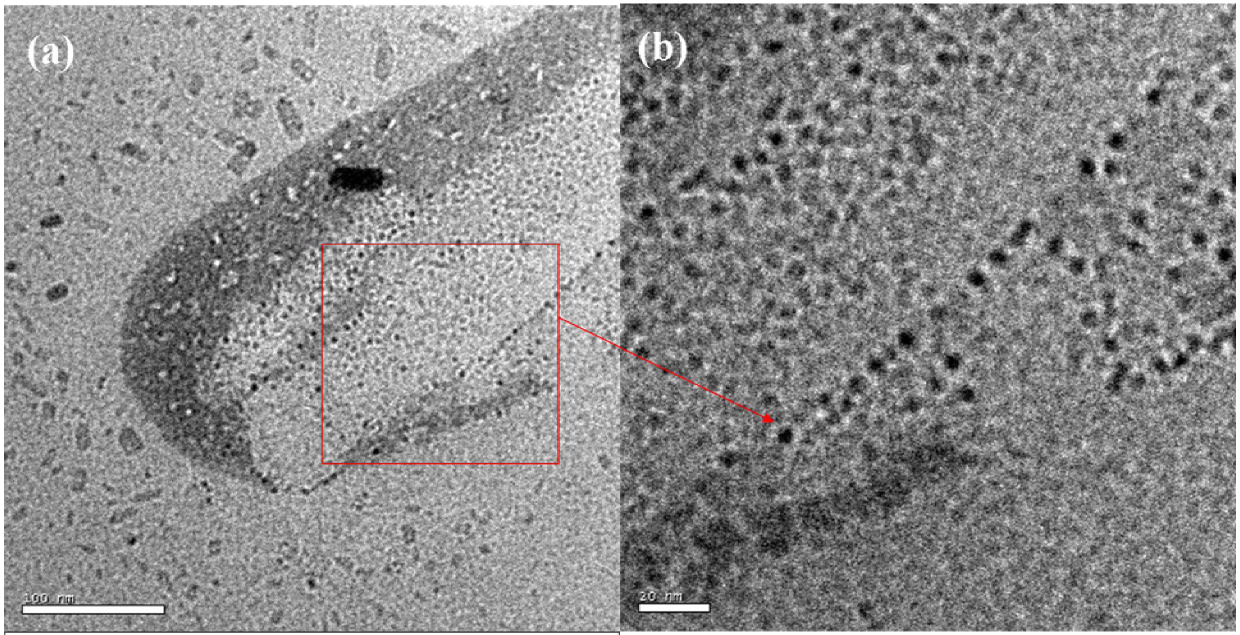

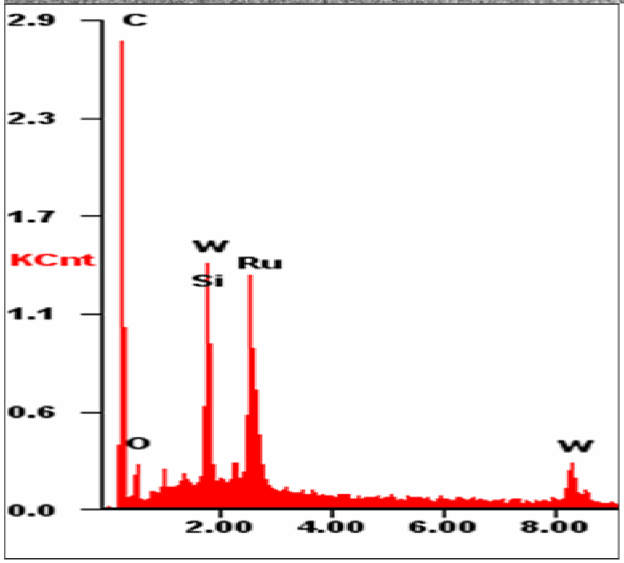

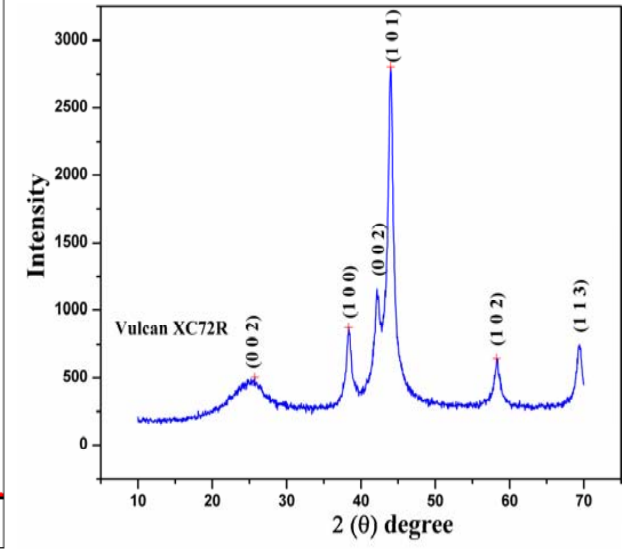

Average particle size of Ru = 3 nm

Synthesis of metal nanoparticles embedded conducting polymer-polyoxometalate nanocomposites

Conducting polymer nanocomposites

Conducting polymer – Metal nanoparticle composites

- Photovoltaic cells
- Memory devices
- Protective coatings against corrosion
- Supercapacitors
- Catalysis

Conducting polymer – Polyoxometalate composites

- Supercapacitors
- Catalysis

Metal nanoparticles – Conducting polymer – Polyoxometalate composites
Further extends composite applications

Synthesis of Conducting polymer-metal nanoparticle Composites

Chemical methods:

- **Reduction of metal salts dissolved in a polymer matrix**
- **Incorporation of preformed nanoparticles during polymerization of monomers**

Electrochemical methods:

- **Incorporation of metal nanoparticles during the electro-synthesis of the polymer**
- **Electrodeposition of metal nanoparticles on preformed polymer electrodes**

Creation of ideal reaction conditions for the simultaneous reactions (polymerization and nanoparticle formation) is a challenge

POM mediated synthesis of conducting polymer- metal nanoparticle composites

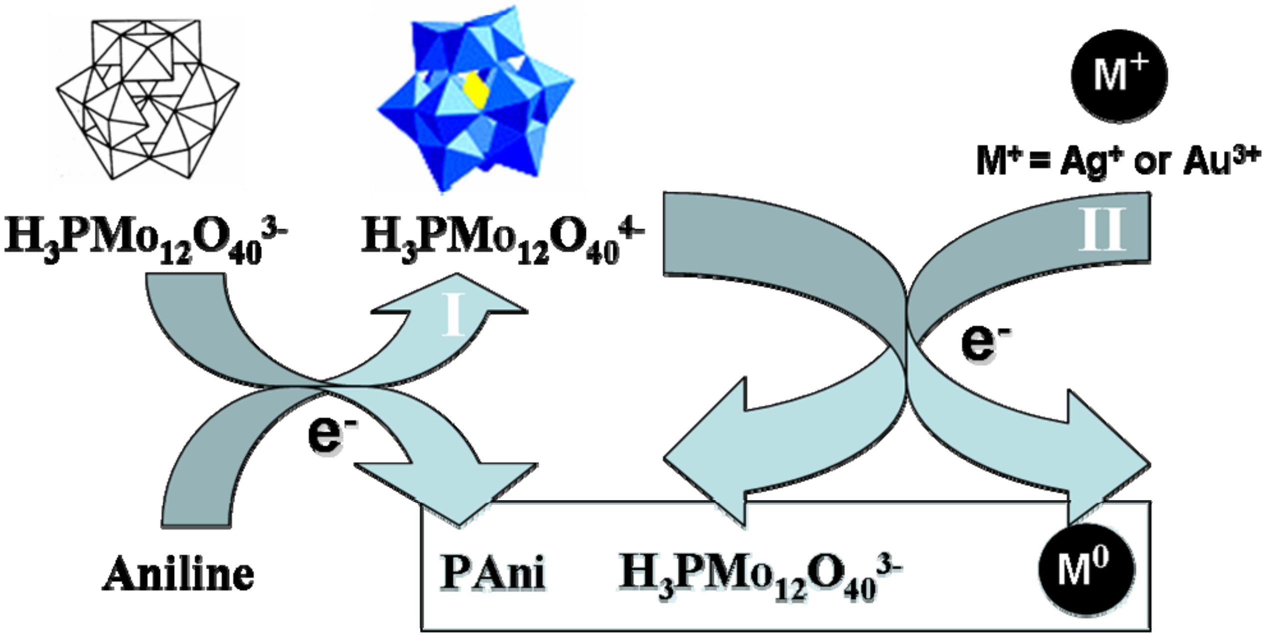

Schematic representation

I Formation of reduced PMo_{12} during polymeriztion of aniline

II Electron transfer from reduced PMo_{12} to metal ions

UV-Vis and XRD analysis of Ag-PAni-PMo_{12} and Au-PAni-PMo_{12} composites

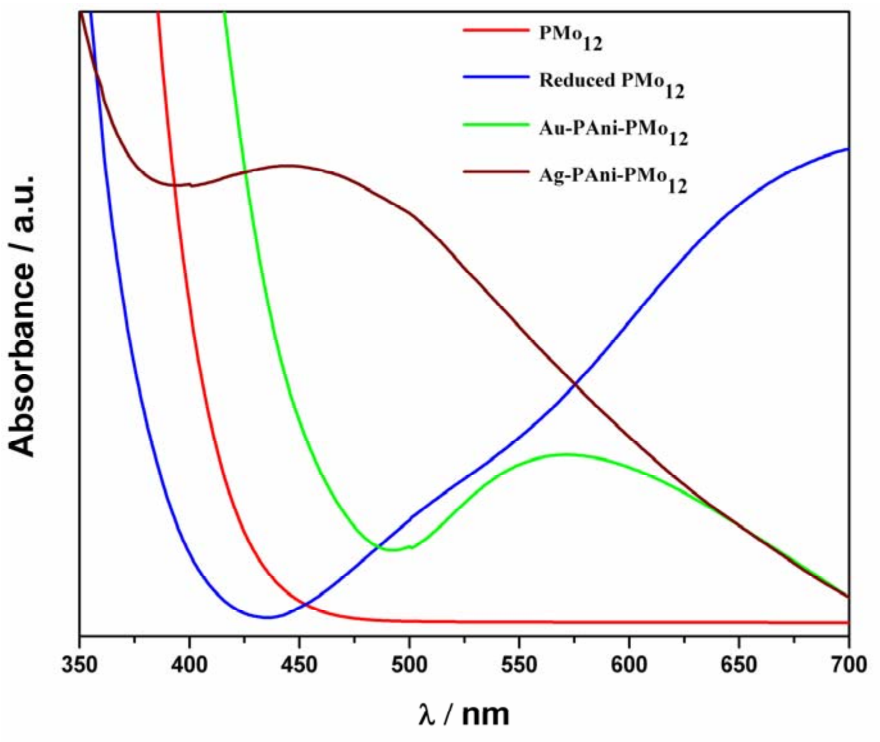

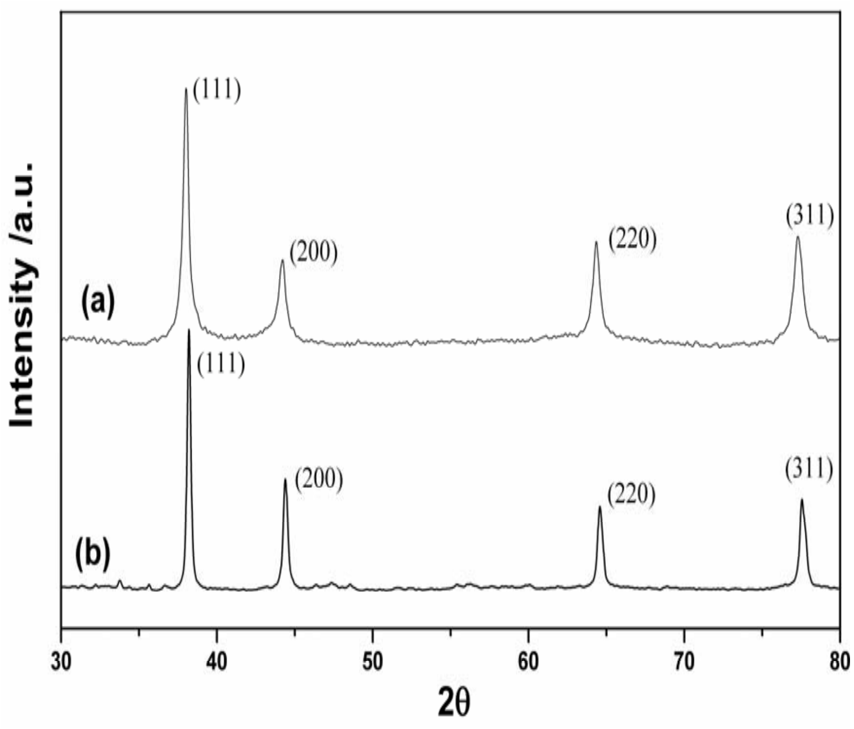

(a) 10 mM PMo_{12}

(b) Mixuture of 5mM PMo_{12} and 20μl of aniline

(c) After addition of 10 mM $AgNO_3$

(d) After adition of 10 mM $HAuCl_4$

(a) Ag-PANi-PMo_{12}

(b) Au-PANi-PMo_{12}

FTIR analysis of Ag-PAni-PMo_{12} and Au-PAni-PMo_{12} composites

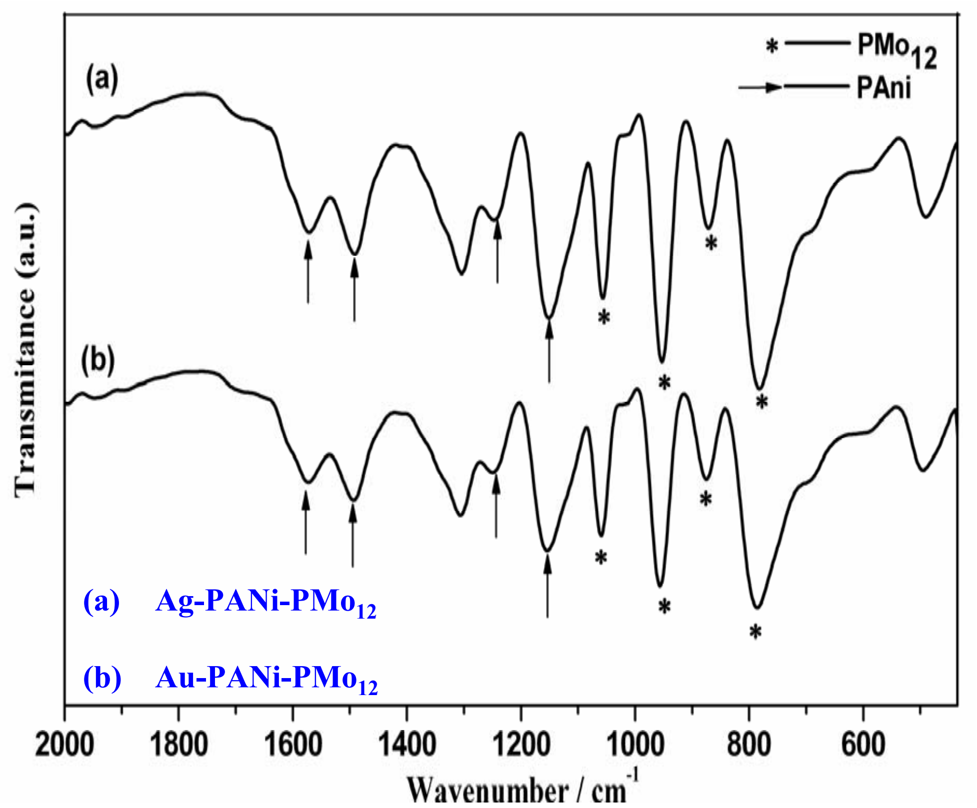

PANI

1575 cm^{-1} deformation mode of benzene rings

1488 cm-1 deformation of quinonoid rings

1248 and 1147 cm^{-1} : C = N str of 2° amine

POM

1060 cm^{-1} : P-O bond

955 cm^{-1} : Mo=O terminal bond

876 cm^{-1} : vertex Mo-O-Mo bond

800 cm^{-1} : Mo-O-Mo bond

SEM images of Ag-PAni-PMo$_{12}$ and Au-PAni-PMo$_{12}$ composites

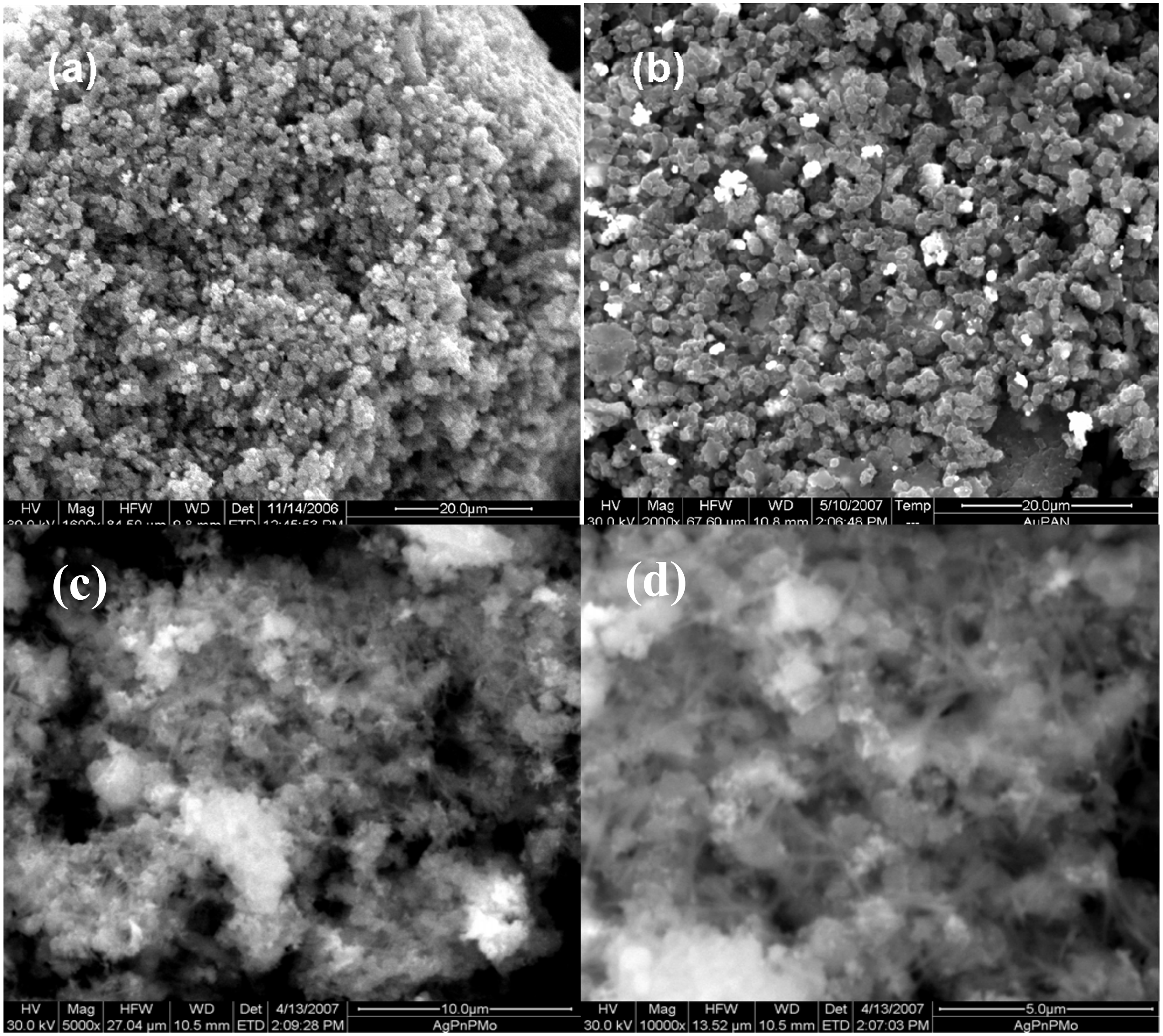

(a) & (b) Ag-Pani-PMo$_{12}$; (c) & (d) Au-PAni-PMo$_{12}$

TEM images of Ag-PAni-PMo_{12} and Au-PAni-PMo_{12} composites

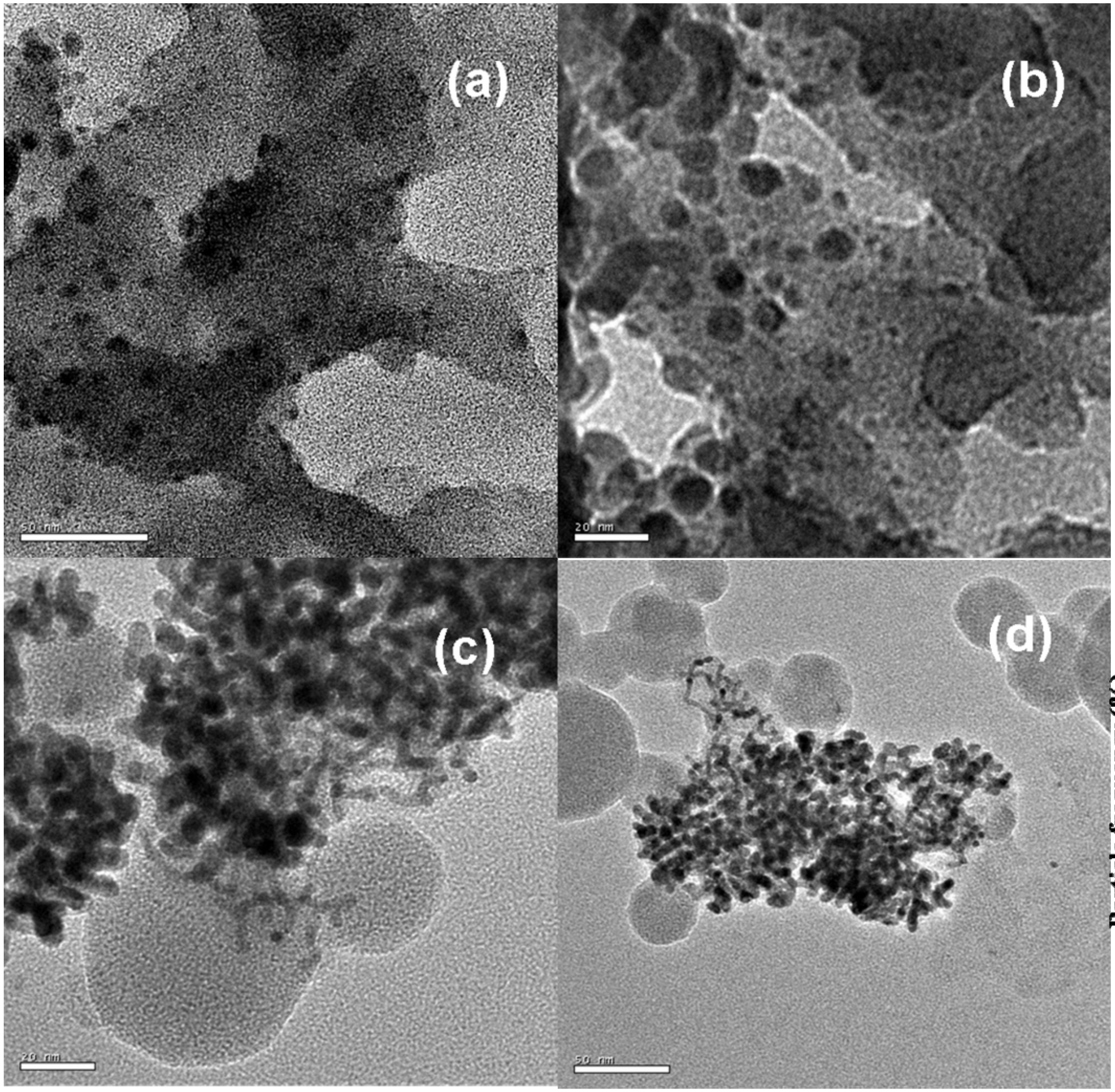

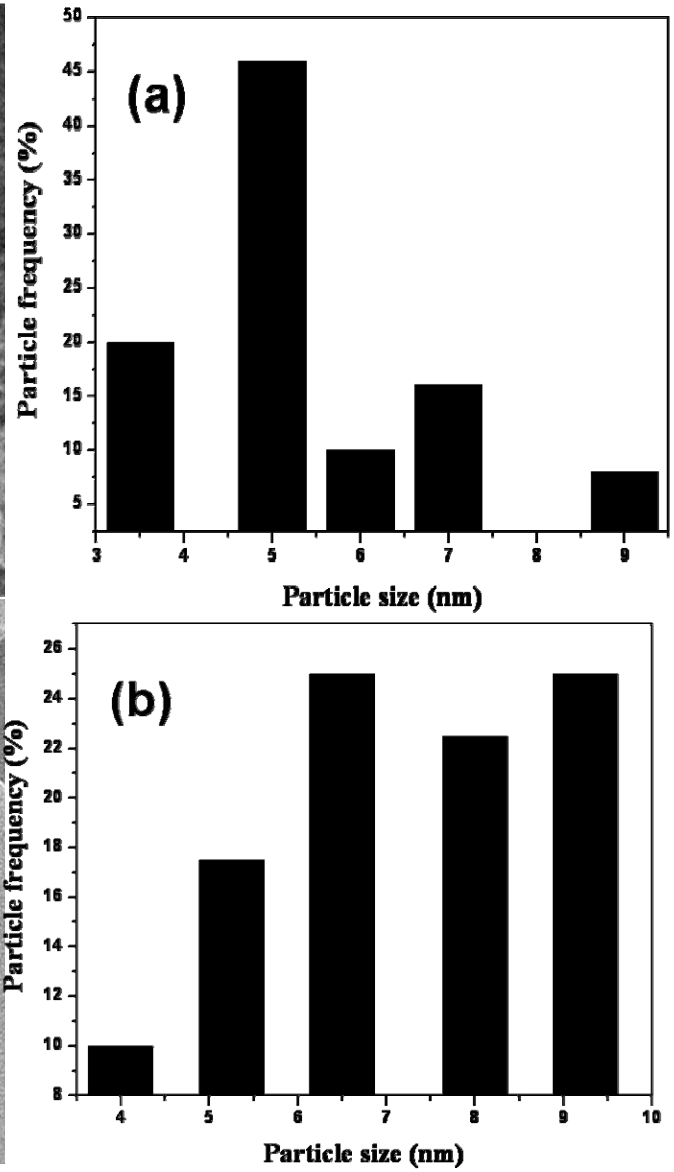

(a) & (b) Ag-Pani-PMo_{12} ; (c) & (d) Au-PAni-PMo_{12}

HRTEM analysis - Formation of core –shell nanoparticles

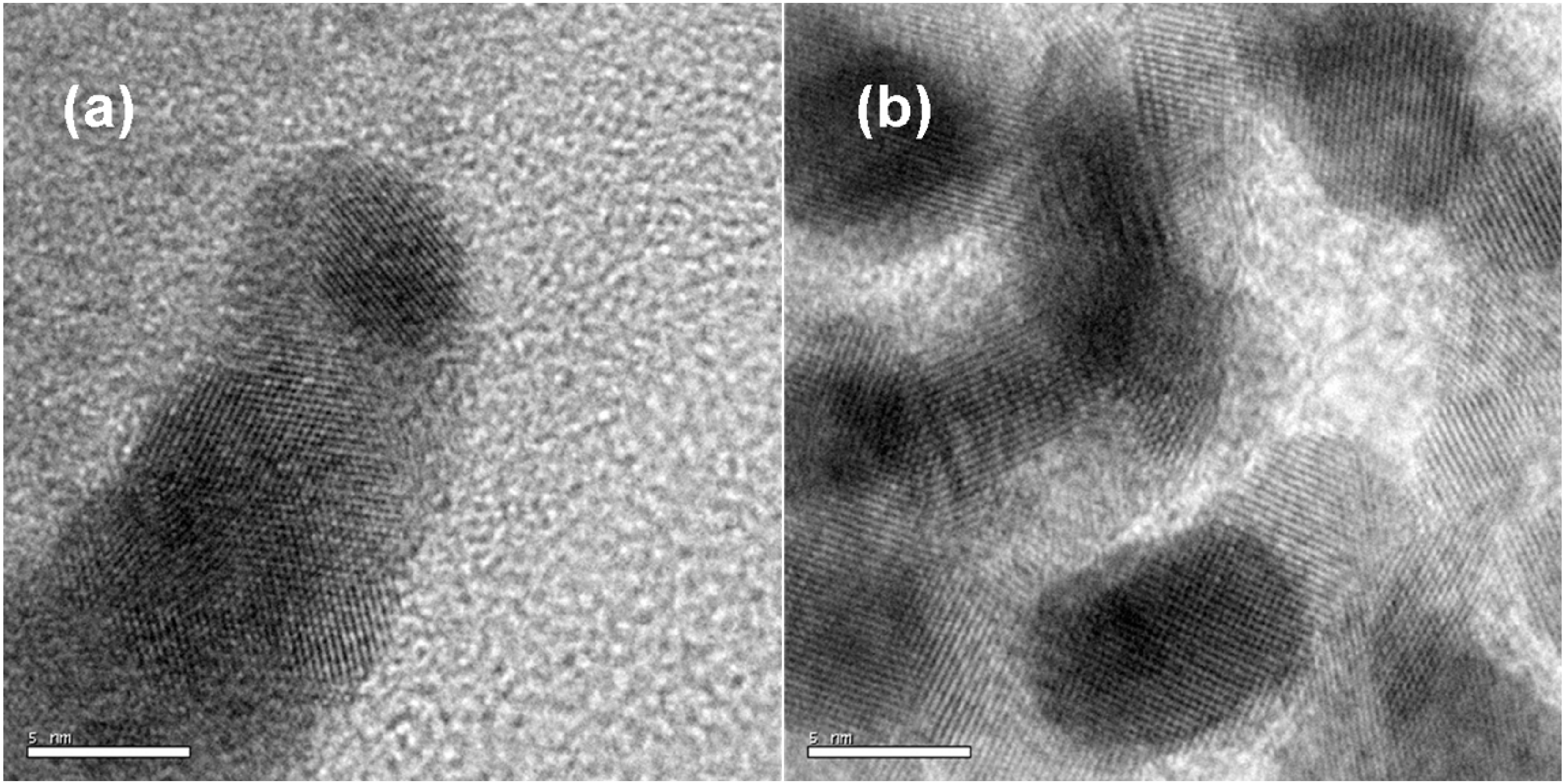

(a) Ag-PANi-PMo$_{12}$

(b) Au-PANi-PMo$_{12}$

- Demonstrates a simple method for Ag and Au nanoparticles embedded in PAni-PMo_{12} nanocomposite
- PMo_{12} has served dual role (oxidizing agent and reducing agent) in the formation of nanocomposite
- The synthesized nanocomposites have core-shell structure with metal nanoparticles being the core and polymer as the shell

Ru/STA-C for electrochemical supercapacitor applications

Electrochemical supercapacitors

- Store or release energy very quickly
- Withstand a large number of charge/discharge cycle
- Operate over a wide range of temperatures
- High market value in memory protection devices
- Low-emission electric vehicles

Metal oxides – Attractive materials for supercapacitors

- Low resistance
- Charging and discharging facilitated by multiple redox states – Faradaic process
- High specific capacitance

Electrochemical supercapacitors

- Store or release energy very quickly
- Withstand a large number of charge/discharge cycle
- Operate over a wide range of temperatures
- High market value in memory protection devices
- Low-emission electric vehicles

Metal oxides – Attractive materials for supercapacitors

- Low resistance
- Charging and discharging facilitated by multiple redox states – Faradaic process
- High specific capacitance

High specific capacitance by RuO_2

- The highest capacitance experimentally reported for RuO_2 is 768 F g^{-1}
- Good electrochemical cyclability
- Provides facile transport pathways for both protons and electrons
- Total specific capacitance per Ru – Expensive
- Effective utilization of Ru with lower loadings is needed
- Employing RuO_2 nanoparticles

Polyoxometalates

- High proton conductivity
- Fast and reversible multi-electron transfer
- Provides additional redox centers

Ru/STA-C for supercapacitor applications

- Preparation of Ru/STA-C composite using silicotungstic acid (STA) as reducing agent
- Variation of Ruthenium loading from 10 - 40 % (wt%)
- Fabrication of electrochemical supercapacitor electrode
- Cyclic Voltammetry studies of Ru/STA-C
- Charge-Discharge characteristics of Ru-STAC using chronopotentiometry
- Comparison of the activities and stabilities of 10% Ru-SiW_{12}/C, 20% Ru-SiW_{12}/C and 40% Ru-SiW_{12}/C has been done in comparison with STA free Ru/C composites

Preparation of Ru/STA-C and Ru/C composites

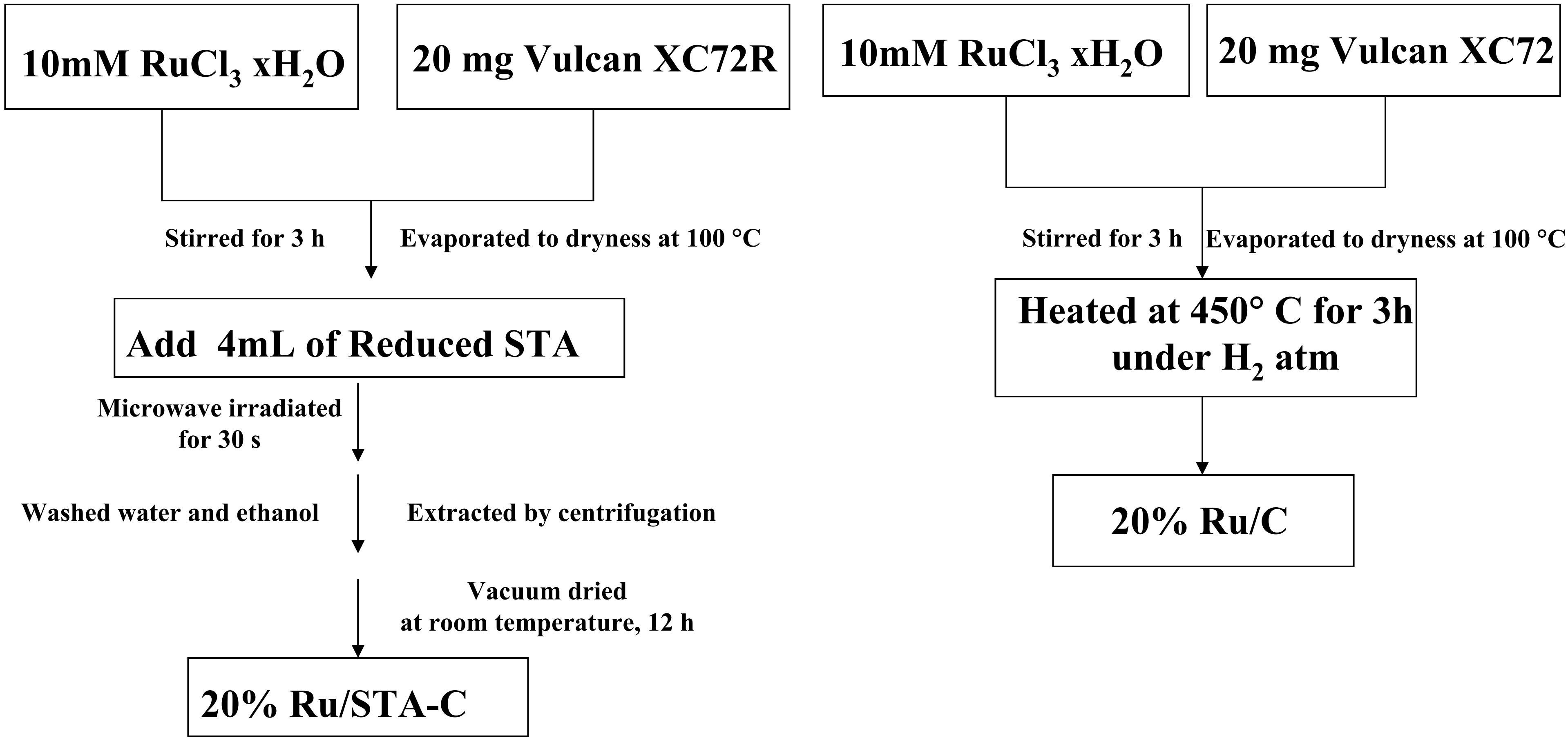

10mM RuCl$_3$ xH$_2$O

20 mg Vulcan XC72R

Stirred for 3 h

Evaporated to dryness at 100 °C

Add 4mL of Reduced STA

Microwave irradiated for 30 s

Washed water and ethanol

Extracted by centrifugation

Vacuum dried at room temperature, 12 h

20% Ru/STA-C

10mM RuCl$_3$ xH$_2$O

20 mg Vulcan XC72

Stirred for 3 h

Evaporated to dryness at 100 °C

Heated at 450° C for 3h under H$_2$ atm

20% Ru/C

Overlay of cyclic voltammograms of RuO_2/STA-C with different RuO_2 loadings

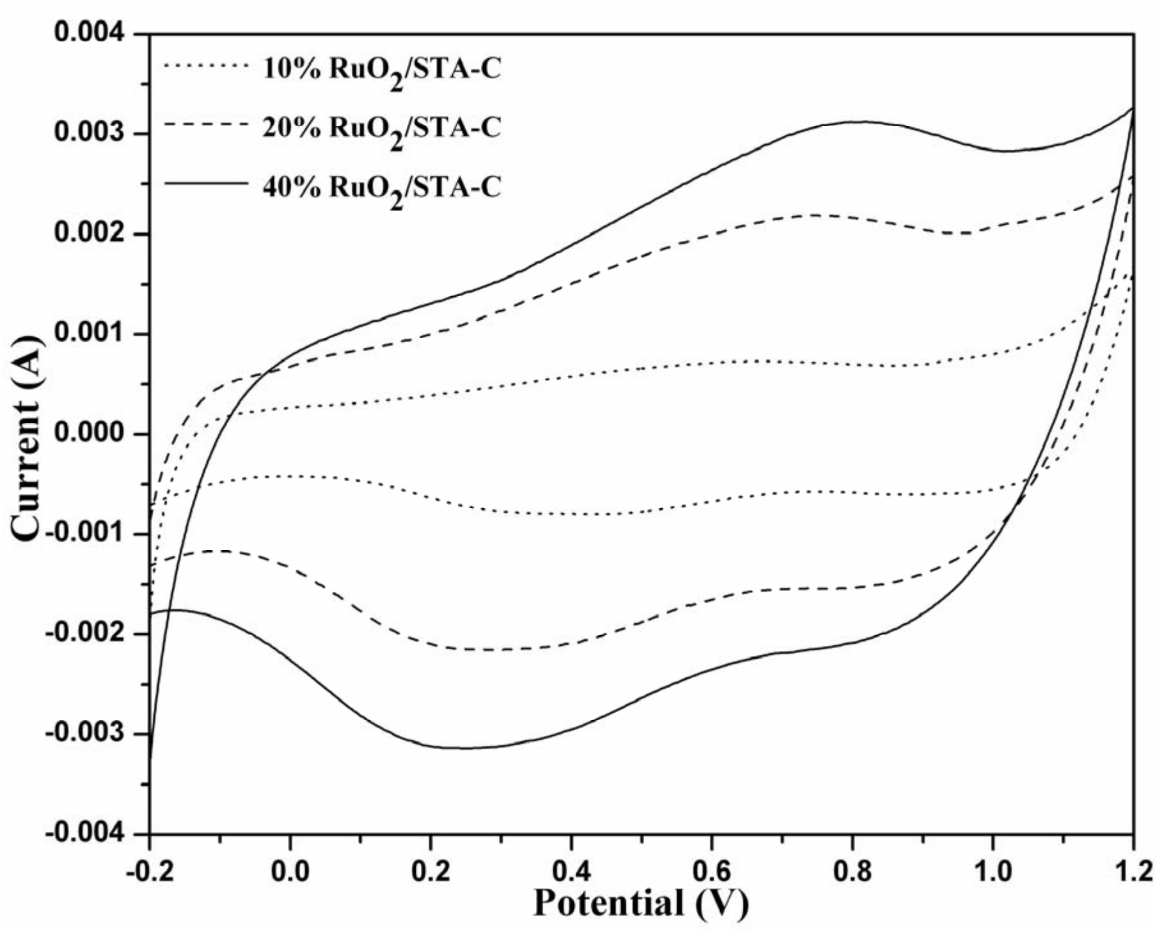

Charge accumulation with increase in RuO_2 percentage

Charge-discharge profiles of vulcan carbon and RuO_2/STA-C composites

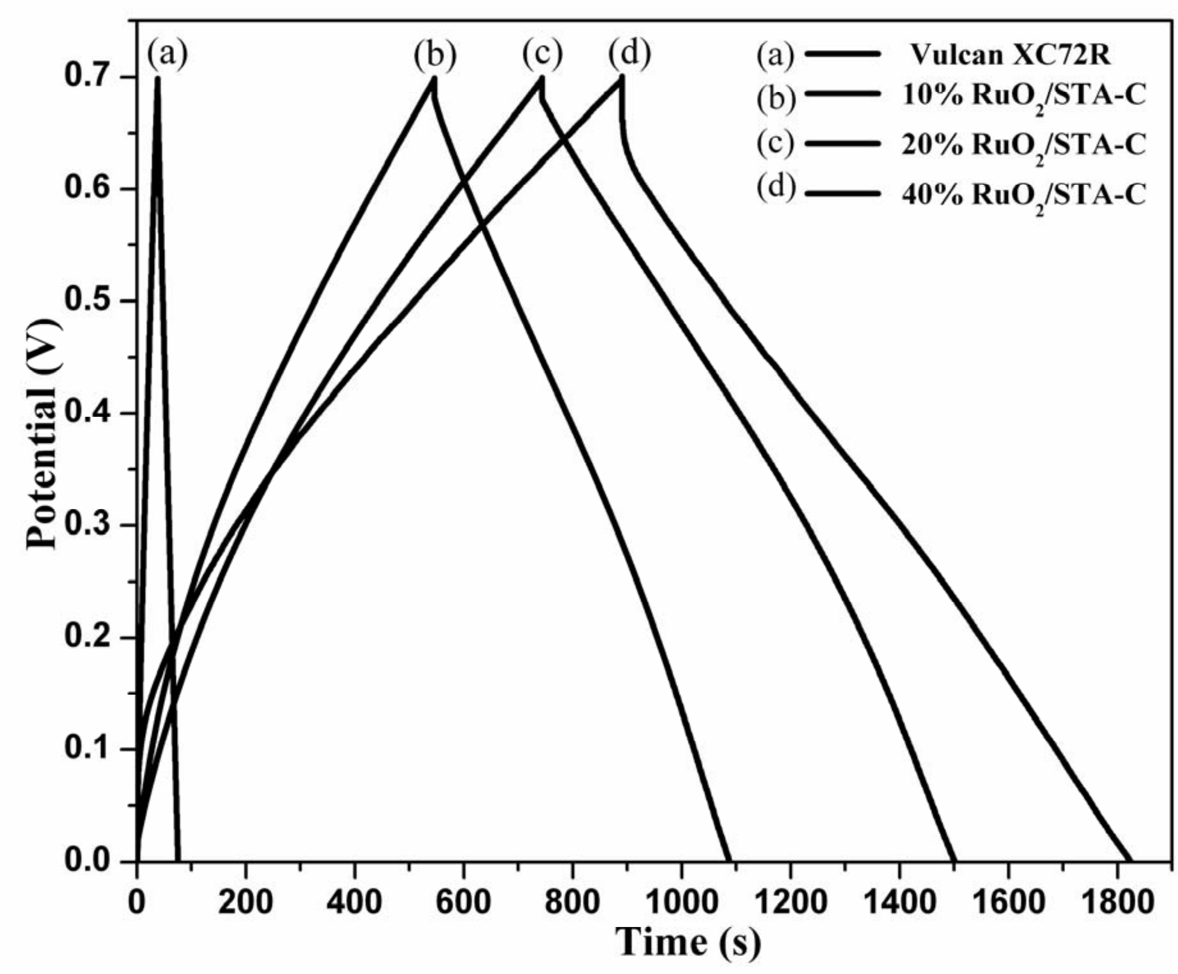

Electrolyte : **1M H_2SO_4**
Applied current : **3 $mAcm^{-2}$**
Potential range : **0.0 – 0.7 V**

Comparison of Charge-discharge curves of 20% RuO_2/STA-C and 20% RuO_2/C for 40 cylces

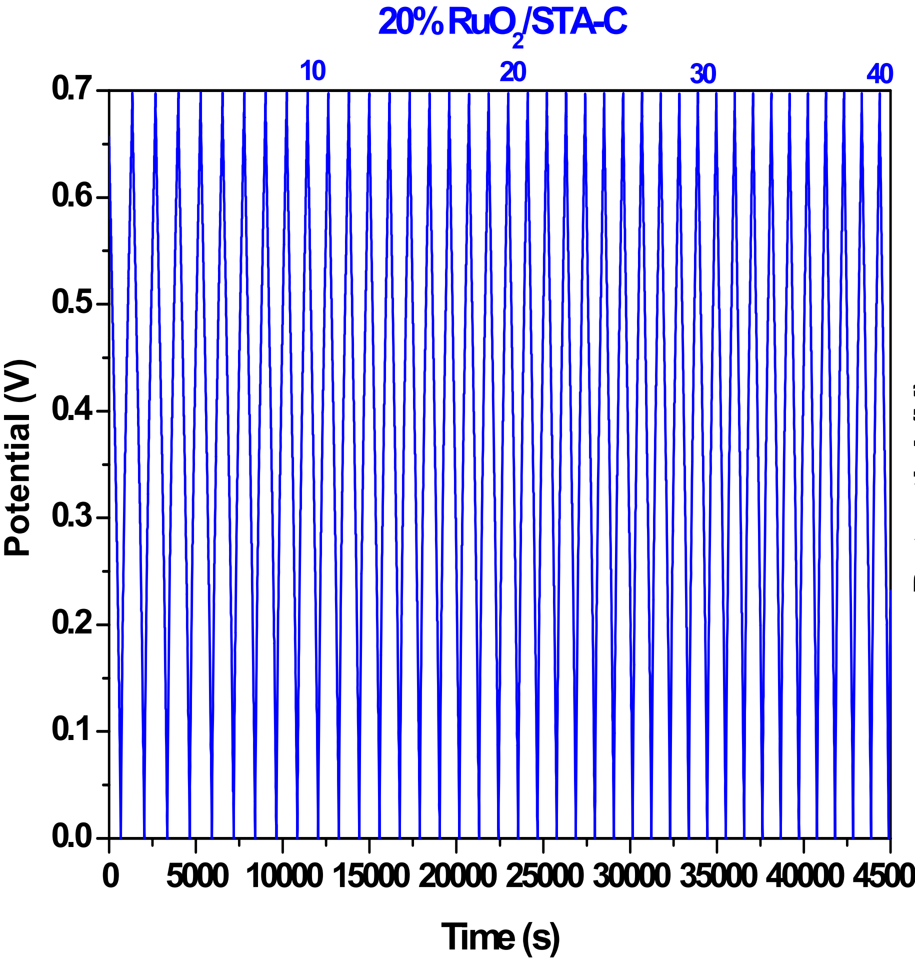

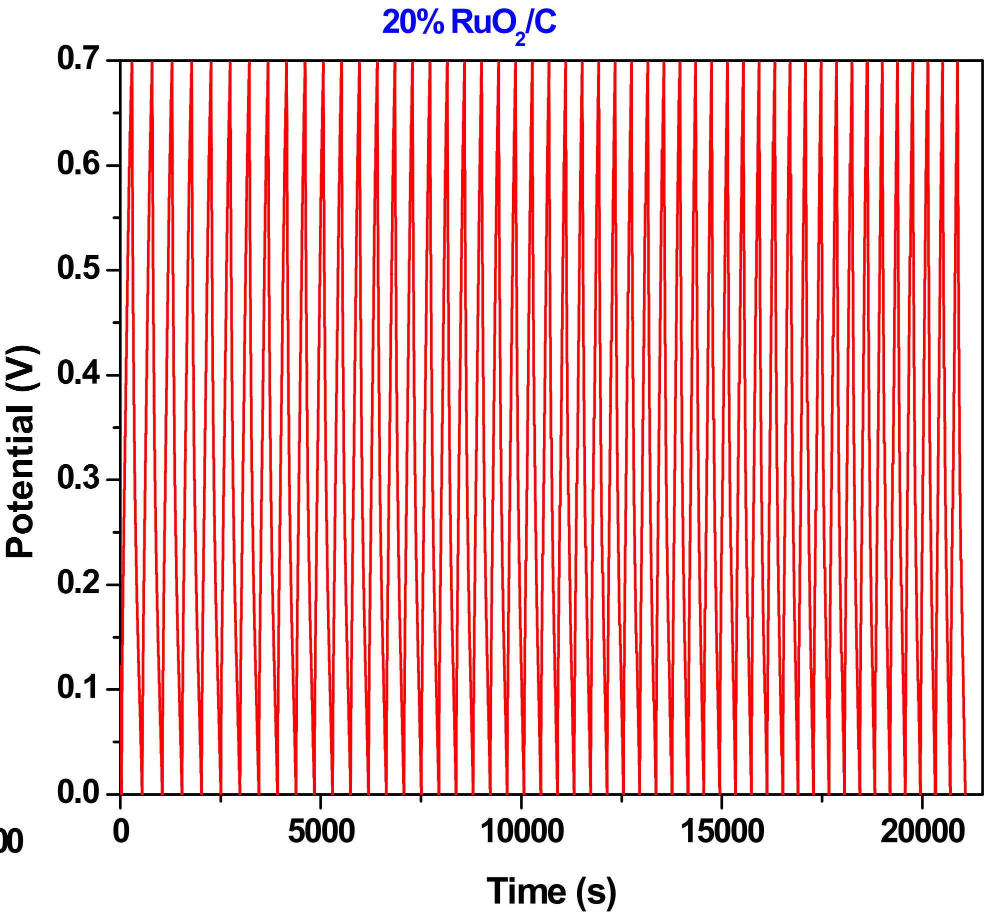

Electrolyte : 1M H_2SO_4
Applied current : 3 $mAcm^{-2}$
Potential range : 0.0 – 0.7 V

Comparison of specific capacitance

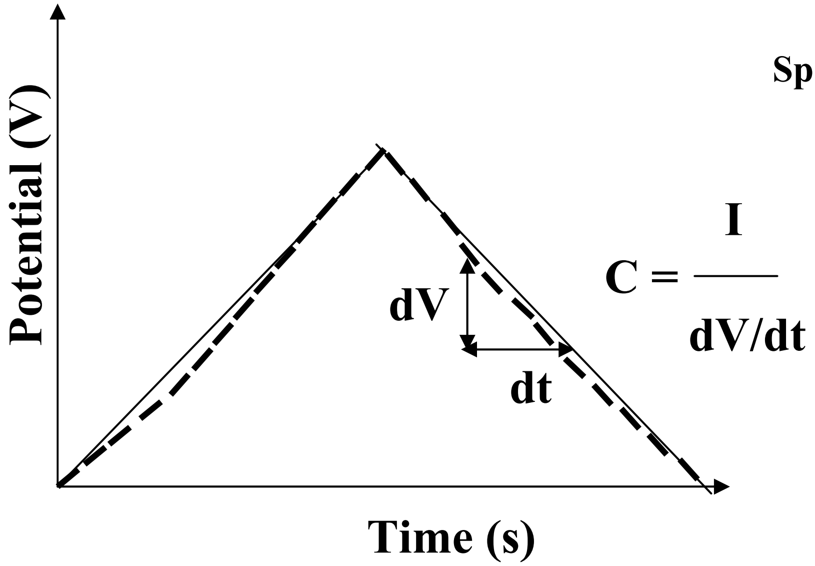

$$C = \frac{I}{dV/dt}$$

Specific Capacitance C (F g^{-1})= I x dt / m x dV

I = Current density in $mAcm^{-2}$
dV = Potential in V
dt = Time in s
m = Weight of the active material in g

S.No	Amount of Ru loaded Wt%	Specific capacitance (F/g)
1	0%(only Vulcan XC72R)	23
2	10% RuO_2/STA-C	325
3	20% RuO_2/STA-C	453
4	20% RuO_2/C	109
4	40% RuO_2/STA-C	557

Specific capacitance Vs Cycle number for RuO_2/STA-C and RuO_2/C

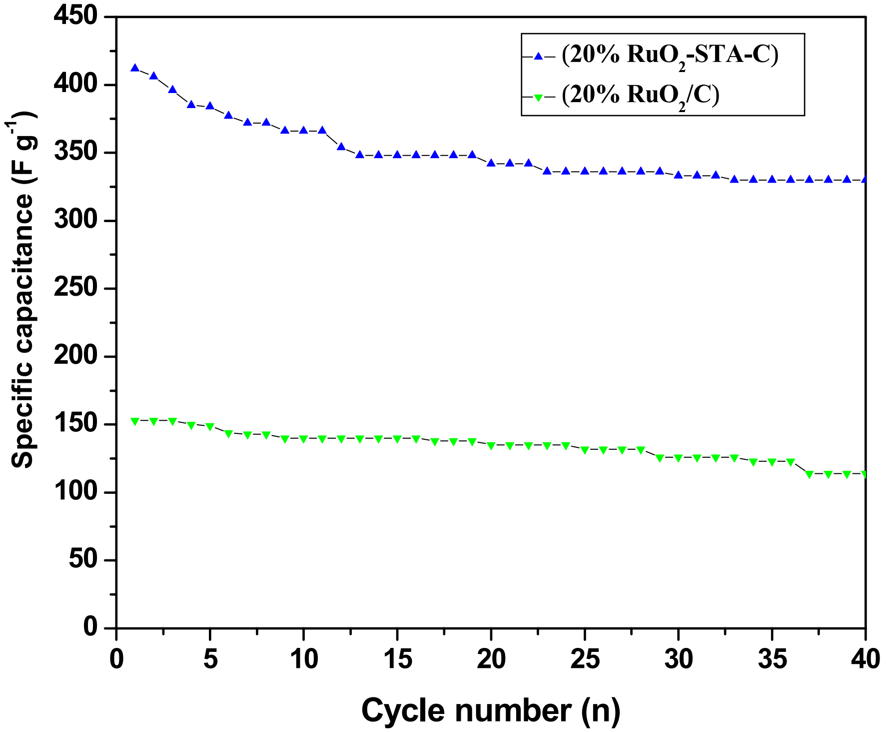

- A simple and efficient method has been developed for the preparation of Ru/POM-C based composite electrode for electrochemical supercapacitor applications
- Presence of polyoxometalate along with RuO_2 in the composite has showed better performance for supercapacitor electrode applications
- Specific capacitance can be increased by altering the ruthenium percentage in the composites
- In this attempt we have improved the performance by reducing the loading of Ru

Application of POM containing carbon supported metal nanoparticles
In
Fuel cells as electrocatalysts

Direct methanol Fuel cells

Anode Reaction : $CH_3OH + H_2O \longrightarrow CO_2 + 6H^+ + 6e^-$

Cathode Reaction : $3/2\ O_2 + 6\ H^+ + 6e^- \longrightarrow 3\ H_2O$

Overall Cell Reaction : $CH_3OH + 3/2\ O_2 \longrightarrow CO_2 + 2\ H_2O$

Efficient anode elctrocatalyst –Pt

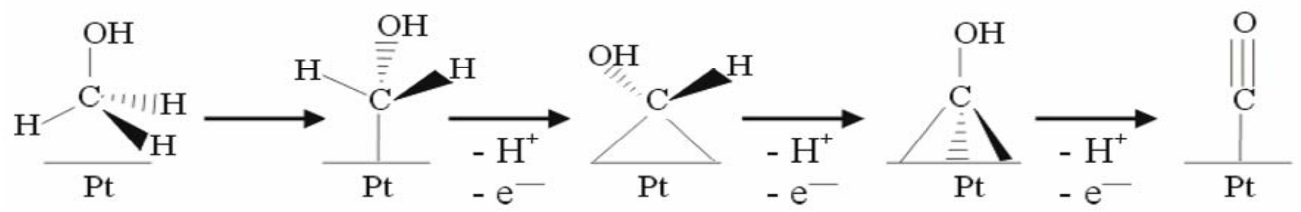

CO adsorption –Shortcomings:

- **Inhibits further methanol adsorption**
- **Induces large overpotential**
- **Requires large currents for CO electro-oxidation to make Pt sites free from CO**
- **Modification of Pt is necessary to enhance the activity**

Can POMs enhance the catalytic activity of noble metals in fuel cell electrodes ?

- **Stable at elevated temperatures**
- **Highly stable in acidic environments**
- **Provides similar environment as that of WO_3 around Pt active sites**
- **Exhibits Oxophilic nature – Activates H_2O molecules and adsorbs OH**
- **Act as mixed electron/proton conductors**
- **POMs on carbon supported gold nanoparticles – served as an efficient CO oxidation catalyst**

$$\mathbf{CO_{(g)} + H_2O_{(l)} + PMo_{12}O_{40}{}^{3-}{}_{(aq)} \rightarrow CO_{2\,(g)} + 2H^+_{(aq)} + PMo_{12}O_{40}{}^{5-}{}_{(aq)}}$$

W. B. Kim, T. Voitl, G. J. Rodriguez-Rivera, J. A. Dumesic., *Science*, 305, **(2004)** 1280-1283

H. Nakajima and I. Honma , *Electrochemical and solid state latters*, 7 (6), **(2004)** A135- A137

Objective

Development of anode electrocatalyst for DMFC inorder to

1. Improve activity
2. Reduce loading of high cost Pt
3. Increase stebility

Development of promoters for reducing CO poisoning

Introduction of promoter (STA) into Pt/C electrocatalyst catalyst

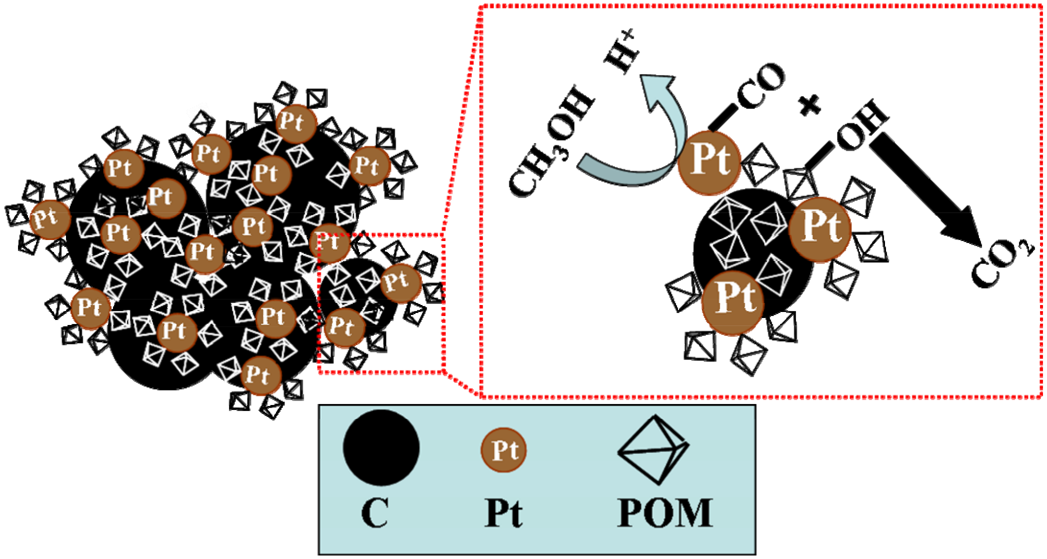

POM containing and POM free Pt/C and Pt-Ru/C carbon electrocatalysts for CH_3OH oxidation

- **Preparation of POM electrocatalysts**
- **20% Pt/STA-C and 20% PtRu/STA-C using $H_4SiW_{12}O_{40}$ (STA)**
- **Preparation of POM free 20%Pt/C and 20%Pt-Ru/C by H_2 reduction method**
- **Comparison of the electrocatalytic methanol oxidation activities of**
  (i) 20% Pt/C (reduced by H_2)
  (ii) 20% Pt/STA-C (reduced by POM)
- **Comparison of the electrocatalytic methanol oxidation activities of**
  (i) 20% PtRu/C (reduced by H_2)
  (ii) 20% PtRu/STA-C (reduced by POM)
  (iii) 20% PtRu/C (J. M) Johnson Matthey (Commercial Catalyst)

20% Pt/STA-C

10mM H_2PtCl_6

Vulcan XC72

↓ Stirred for 3 h

↓ Evaporated to dryness

Add 4mL of Reduced STA

↓ Microwave irradiation for 30 sec

↓ Washed with H_20 & centrifuged

↓ Dried

20% Pt/C

20% Pt-Ru/STA-C

10mM H_2PtCl_6

10mM $RuCl_3$

Vulcan XC72

↓ Stirred for 3 h

↓ Evaporated to dryness

Add 4mL of reduced STA

↓ Microwave irradiation for 30 sec

↓ Washed with H_20 & centrifuged

↓ Dried

20% PtRu/C

20% Pt/C

10mM $H_2PtCl)$

Vulcan XC72

↓ Stirred for 3 h

↓ Evaporated to dryness

Heated at 450° C for 4h in H_2 Atm

↓

20% Pt/C

20% Pt-Ru/C

10mM H_2PtCl_6

10mM $RuCl_3$

20 mg Vulcan XC72

↓ Stirred for 3 h

↓ Evaporated to dryness

Heated at 450° C for 4h in H_2 Atm

↓

20% PtRu/C

FTIR and XRD analysis of the composite electrocatalysts

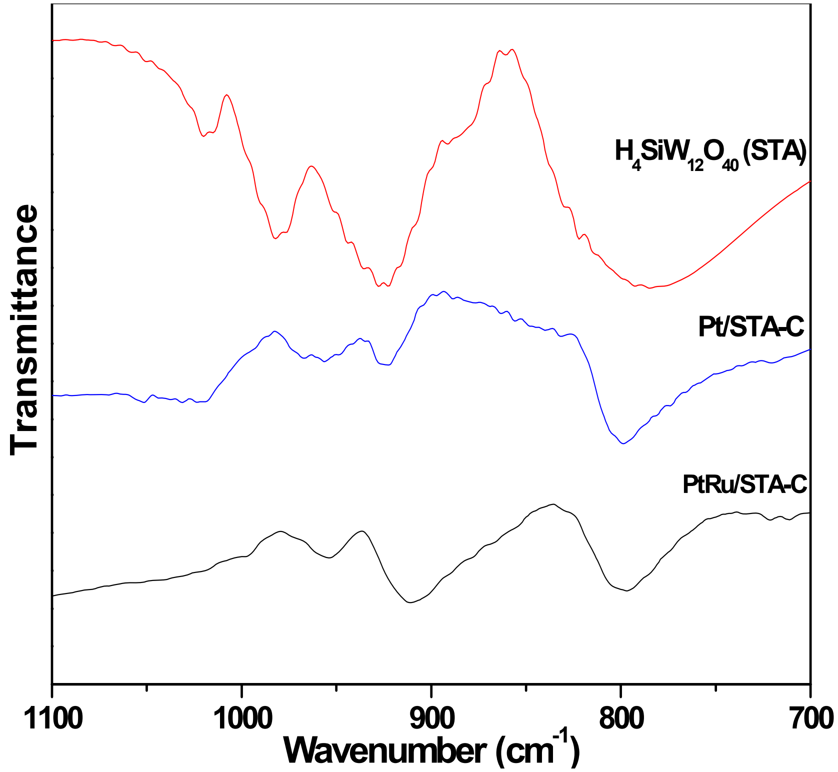

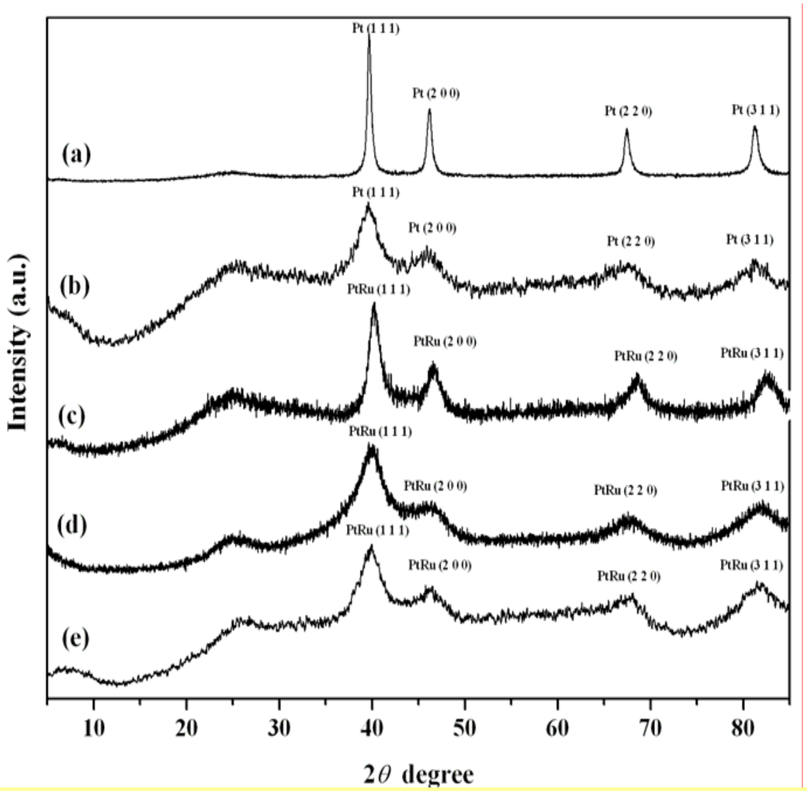

Shift in the band frequencies confirms
-chemisorption of POMs on carbon surface

Peak broadening in POM reduced Pt/STA-C and PtRu/STA-C confirms the reduction in particle size

Frequency (υ) cm^{-1}	$H_4SiW_{12}O_{40}$	PtRu/STA-C	Pt/STA-C
(W=O_t)	980	955	957
(Si-O)	926	911	924
(W-O_e-W)	784	798	798

(a) Pt/C & (c) PtRu/C (H_2 reduction method)

(b) Pt/STA-C & (d) PtRu/STA-C (POM reduction method)

(e) PtRu/C (J. M) commercial

TEM and HRTEM analysis of all the composites

TEM images

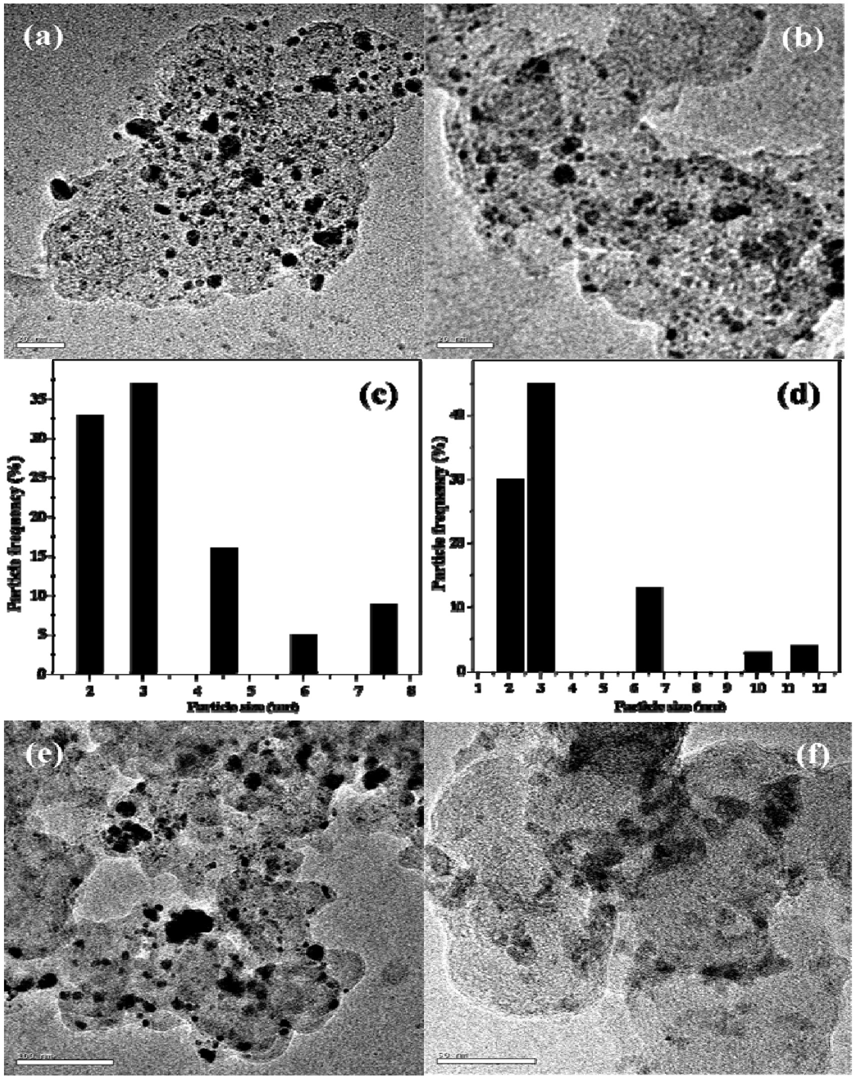

(a) Pt/STA-C (b) PtRu/STA-C ---- Fine distribution of particles
(c) & (d) particle distribution from (a) & (b)
(e) Pt/C (f) PtRu/C (H_2 reduction method) --- Agglomaration of particles

HRTEM images

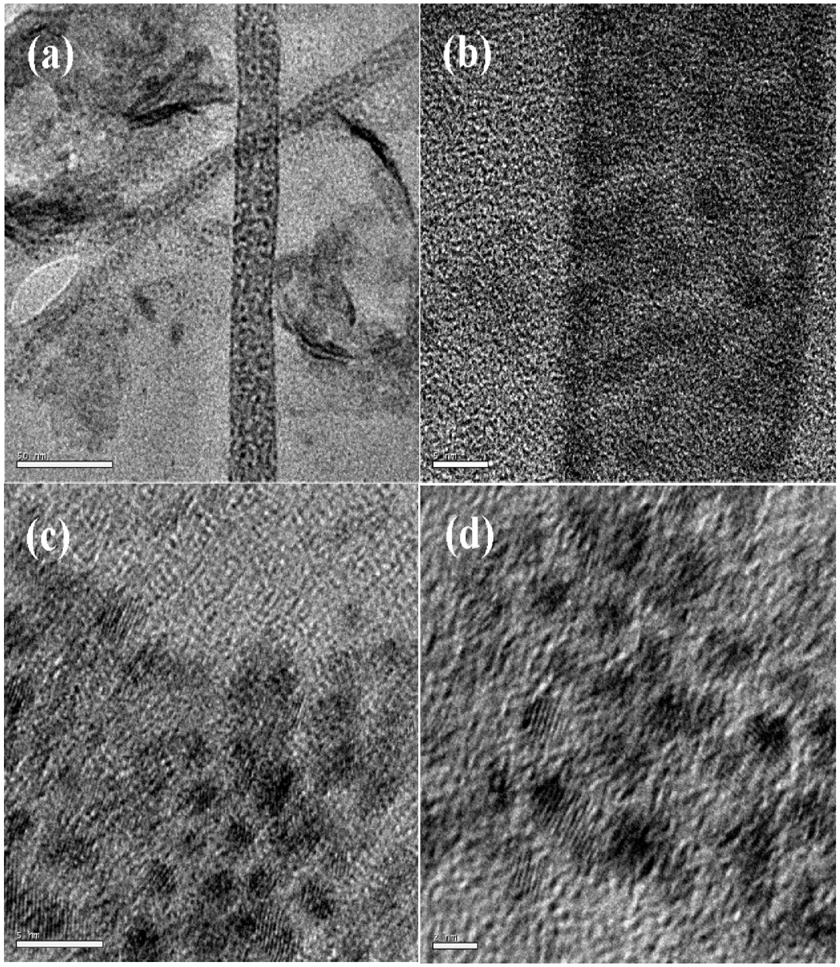

(a) & (b) Pt/STA-C (c)& (d)PtRu/STA-C

Electrochemical active surface area of Pt

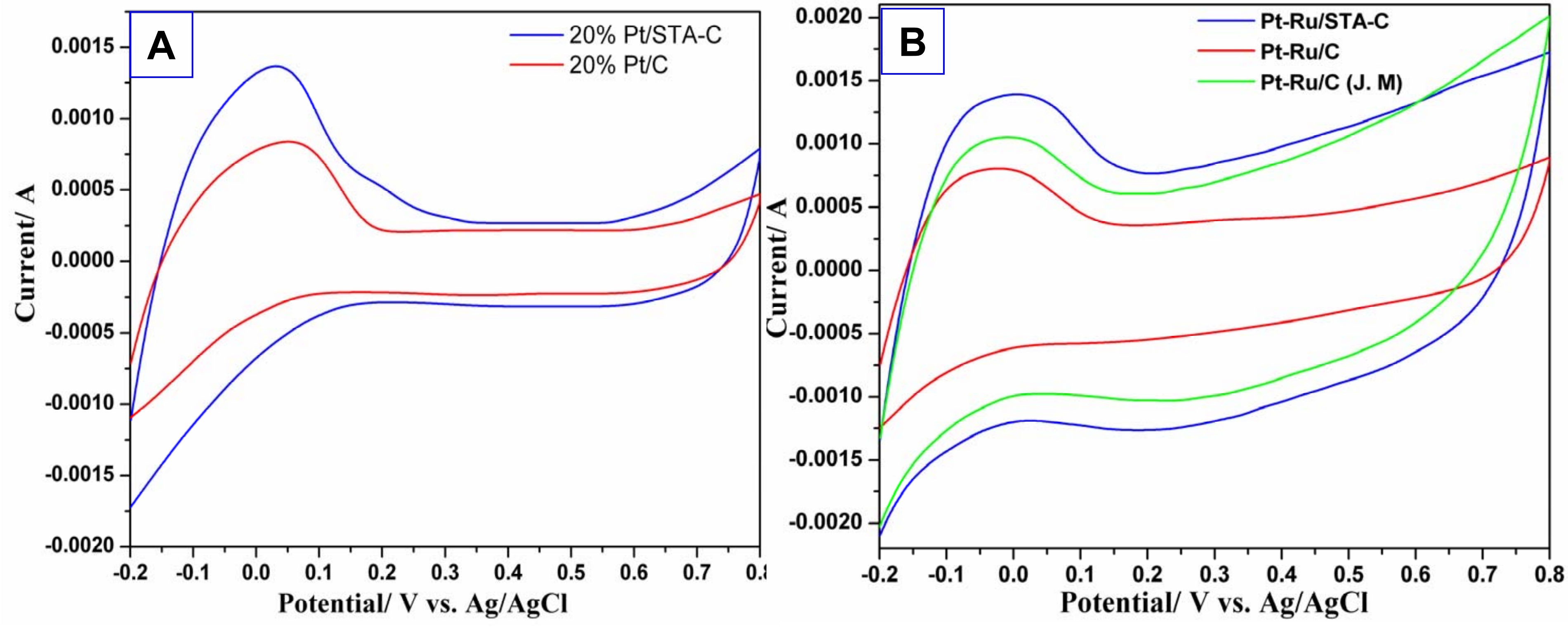

(A) Overlay of cyclic voltammograms of Pt/STA- C and Pt/C (H_2 reduction method)

(B) Overlay of cyclic voltammograms of PtRu/STA- C, PtRu/C (J. M) and PtRu/C)

Electrolyte : 1M H_2SO_4 ; Scan rate: 25mV /s

Improvement in the H adsorption desorption in thr case of STA containing systems confirms the imcrease of electrochemical active surface area

Electrode fabrication

- Three-electrode set up using Pt disk (1cm X 1cm) as counter electrode
- Ag/AgCl/ (sat KCl) as the and reference electrode
- Glassy carbon coated with electrode material as working electrode
- The electrolyte used was 1 M H_2SO_4 at room temperature and geometrical area of electrode = $0.07cm^2$

- 10 mg of 20%Pt/STA-C or 20% Pt/C has been dispersed in 300μL H_2O by sonication
- 10 μL has been coated on GC (0.07 cm2)and dried in an oven at 70° C
- 5 μL of Nafion as a binder and dried at room temperature

Comparison of methanol oxidation activity using Cyclic voltammetry

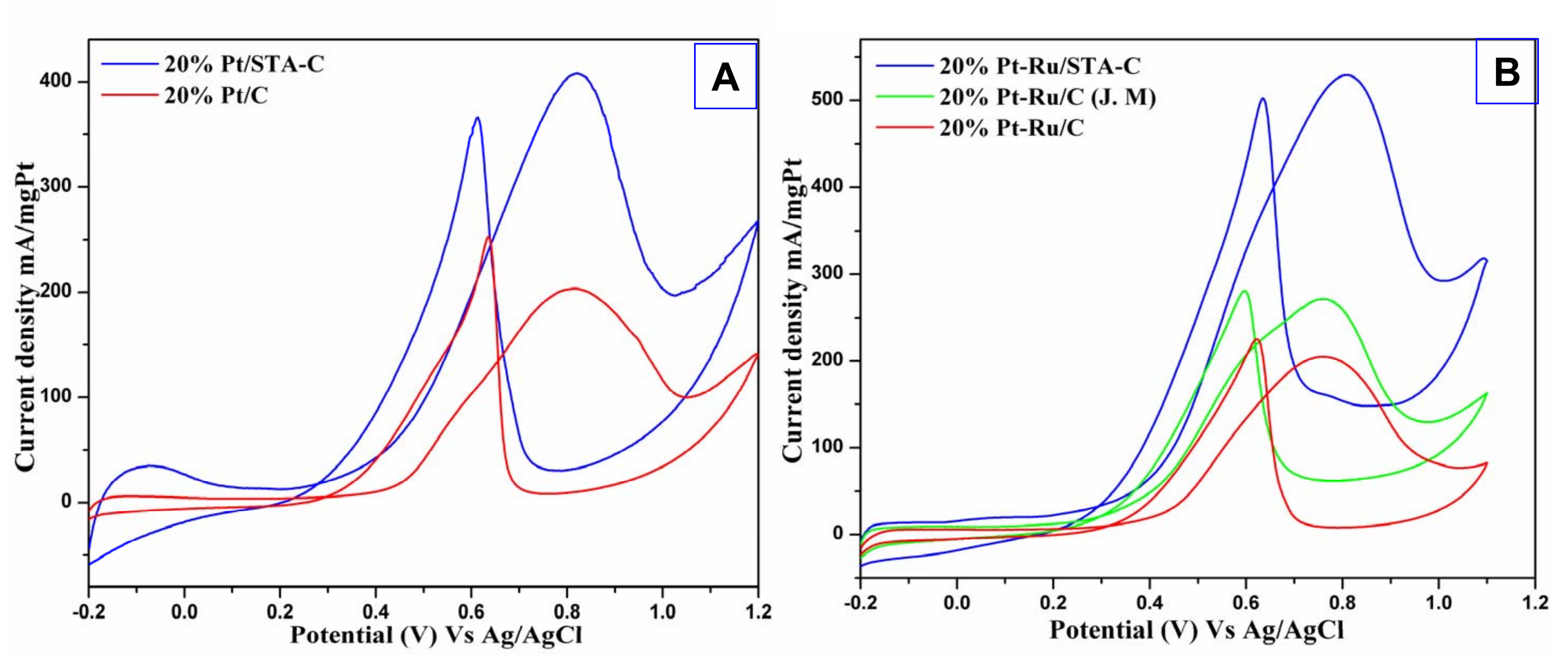

A. Cyclic voltammetric curves overlay of Pt/STA-C and Pt/C

B. Cyclic Voltammetric curves overlay of PtRu/STA-C, PtRu/C (J.M) and PtRu/C

Electrolyte : 1M H_2SO_4 , 1 M CH_3OH ; Scan rate: 25mV /s

Comparison of methanol oxidation activity at 0.75 V using Chronoamperometry

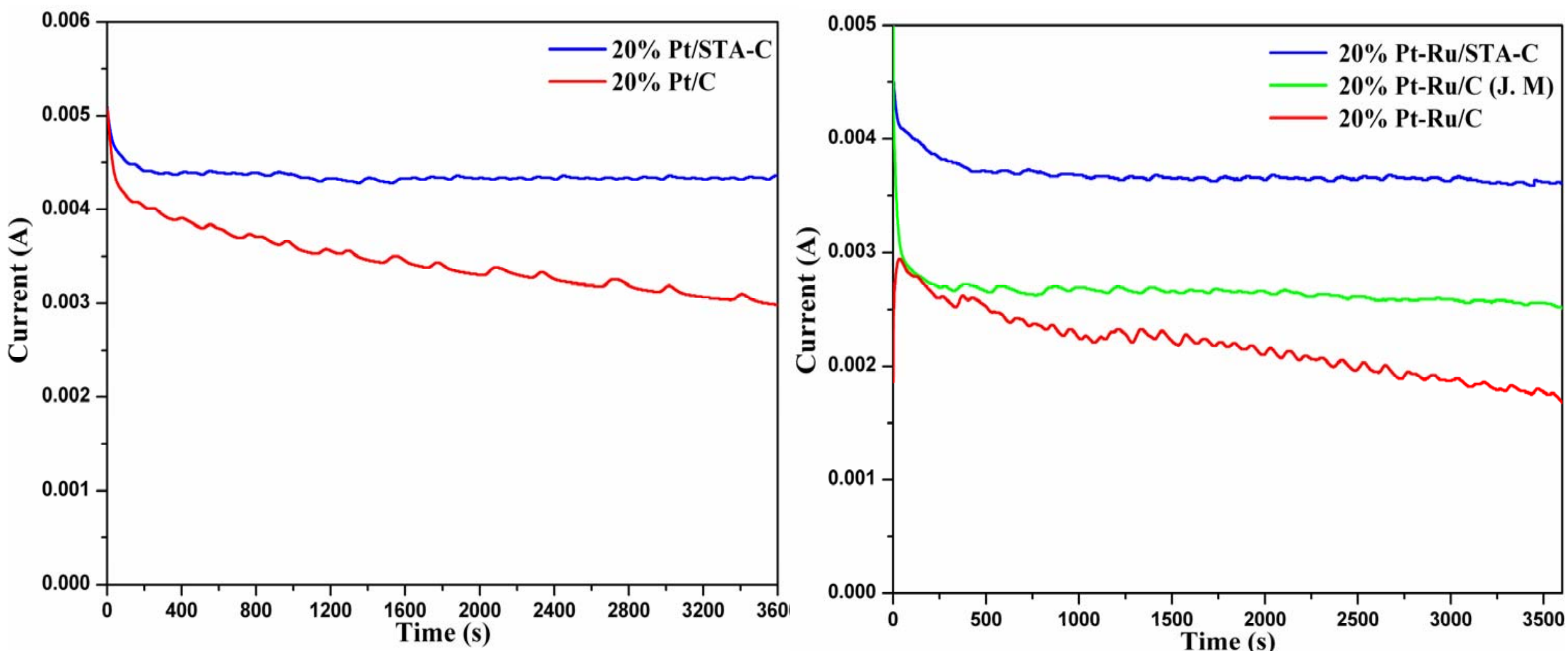

A. Chronoamperometric curves overlay of Pt/STA-C and Pt/C

B. Chronoamperometric curves overlay of PtRu/STA-C, PtRu/C (J.M) and PtRu/C

Electrolyte : 1M H_2SO_4 , 1 M CH_3OH

Effect of POM on Pt/C and Pt-Ru/C towards methanol oxidation

Catalyst	EAS[a] (m^2g^{-1})	Onset Potential (V)	I_f/I_b	Mass Activity ($mAmg^{-1}$ Pt)	Specific Activity ($mAcm^{-2}$ Pt)
Pt/C	23.3	0.31	0.80	191	0.81
Pt/STA-C	33.0	0.21	1.11	370	1.12
Pt-Ru/C	17.2	0.21	0.91	204	1.18
Pt-Ru/STA-C	25.6	0.17	1.05	503	1.96
Pt-Ru/C (J.M)	22.5	0.17	0.95	271	1.20

- I_f/I_b – ratio of forward to reverse peak current - corresponds to tolerance of the catalyst towards CO poisoning
- Higher I_f/I_b value – better tolerance for CO poisoning
- Electrocatalysts reduced by STA showed higher I_f/I_b value
- Onset potential values suggests that the STA reduced catalysts are superior in activity than catalysts prepared by H_2 reduction method
- Both the current density and mass specific activities are higher for STA reduced catalysts
- This can be attributed to the higher electroactive surface area of the STA reduced catalyst
- By chronoamperometry studies it is revealed that the staility of the STA reduced catalyst is higher than H_2 reduced catalyst

Role of Silicotungstic acid (STA)

- Acted as reducing agent to form metal nanoparticles
- Modified the carbon structure into nanometer regime
- The excellent redox properties, and the high electron/proton conductivity of $H_4SiW_{12}O_{40}$ (STA) can increase the conductivity of the electrode and promote electron-transfer reactions
- The oxidation of CO by $H_4SiW_{12}O_{40}$ may diminish the poison of catalysts
- Possible explanation:

  Having in mind that $H_4SiW_{12}O_{40}$ highly symmetrical ensemble reminiscent of its parent metal oxide (WO3), STA has been found to provide similar environment of WO_3 /hydrogen bronze matrices

Enhancement of activity of oxygen reduction reaction
by
Pt/STA-C electrocatalyst

Oxygen reduction reaction (ORR)

$$\begin{tikzcd}
O_2 \arrow[r] & O_{2\ ad} \arrow[r, shift left] \arrow[rr, dashed, bend left] & H_2O_{2\ ad} \arrow[l, shift left] \arrow[r] & H_2O
\end{tikzcd}$$

Indirect pathway

$O_2 + Pt \rightarrow Pt\text{-}O_2$

$Pt\text{-}O_2 + H^+ + 1e^- \rightarrow Pt\text{-}HO_2$

$Pt\text{-}HO_2 + Pt \rightarrow Pt\text{-}OH + Pt\text{-}O$

$Pt\text{-}OH + Pt\text{-}O + 3H^+ + 3e^- \rightarrow 2\ Pt + 2\ H_2O$

- **Pt based catalysts are best employed to have high activity**
- **Formation of H_2O_2 intermediate – Sluggish the performance of Pt**
- **Modification of Pt is necessary**

Activating role of WO_3 in ORR

- **Interacts with Pt via hydrogen spill over and forms highly conductive tungsten oxide bronzes (H_xWO_3)**

$$\text{Pt-H} + WO_3 \rightarrow \text{Pt} + H_xWO3$$

- **Tungsten bronzes are highly reactive towards reduction of H_2O_2 intermediate**
- **Bronzes leads to an increase in overall matrix conductivity (3 orders of increment)**
- **Facilitate electron transfer to three dimensionally dispersed Pt particles**
- **Pt/WO_3 shows appreciable activity towards hydrogen evolution**
- **Provides of charge (electron and proton) propagation**

Anlogously W based nanomaterials compounds which can form
tungsten bronzes in acidic media
improves the efficiency of Pt nanoparticles towards O_2 reduction reaction

P. J. Kulesza and B. Grzybowaska, M. A. Malik and M. T. Galkowski, *J. Electrochem. Soc*., 144, 1997, 1911

W based POM [$H_4SiW_{12}O_{40}$, (STA)] are anologous to WO_3

- POMs can be viewed as nanostructure of parent metal oxides (WO_3) organized around heterogroup (silicate or phosphate)
- Capable of transfer electrons coupled with high reductive reactivity (reduces H_2O_2 effiently)
- Inhers super-acid properties - provides mobility of protons at the lectrocatalytic interface
- Forms electroactive adsorbates on platinum surfaces
- Chemisorb strongly on carbon surfaces

Due to the synergetic effect of Pt and POM, enhanced activity towards O_2 reduction can be achieved

Modification of Pt/C with STA and comparison of activity with STA free Pt/C

1. Preparation of 20% Pt/STA-C using STA as reducing agent
2. Preparation of STA free 20% Pt/C using H_2 reduction method
3. Electrochemical O_2 reduction using 20% Pt/STA-C and 20%Pt/C
4. Comparison of the activities of
    (i) 20% Pt/C reduced by H_2
    (ii) 20% Pt/C reduced by POM

Electrode Fabrication

Electrochemical measurements were carried out using CHI660 electrochemical workstation

- **Three-electrode set up using Pt wire counter electrode**
- **Ag/AgCl/ (sat KCl) as the and reference electrode**
- **Glassy carbon coated with electrode material as working electrode**
- **The electrolyte used was 0.5 M H_2SO_4 at room temperature and geometrical area of electrode = $0.07cm^2$**
- **10 mg of 20%Pt/STA-C or 20% Pt/C has been dispersed in 300µL H_2O by sonication**
- **10 µL has been coated on GC (0.07 cm2)and dried in an oven at 70° C**
- **5 µL of Nafion as a binder and dried at room temperature**

ORR activity for Pt/STA-C by linear sweep voltammetry

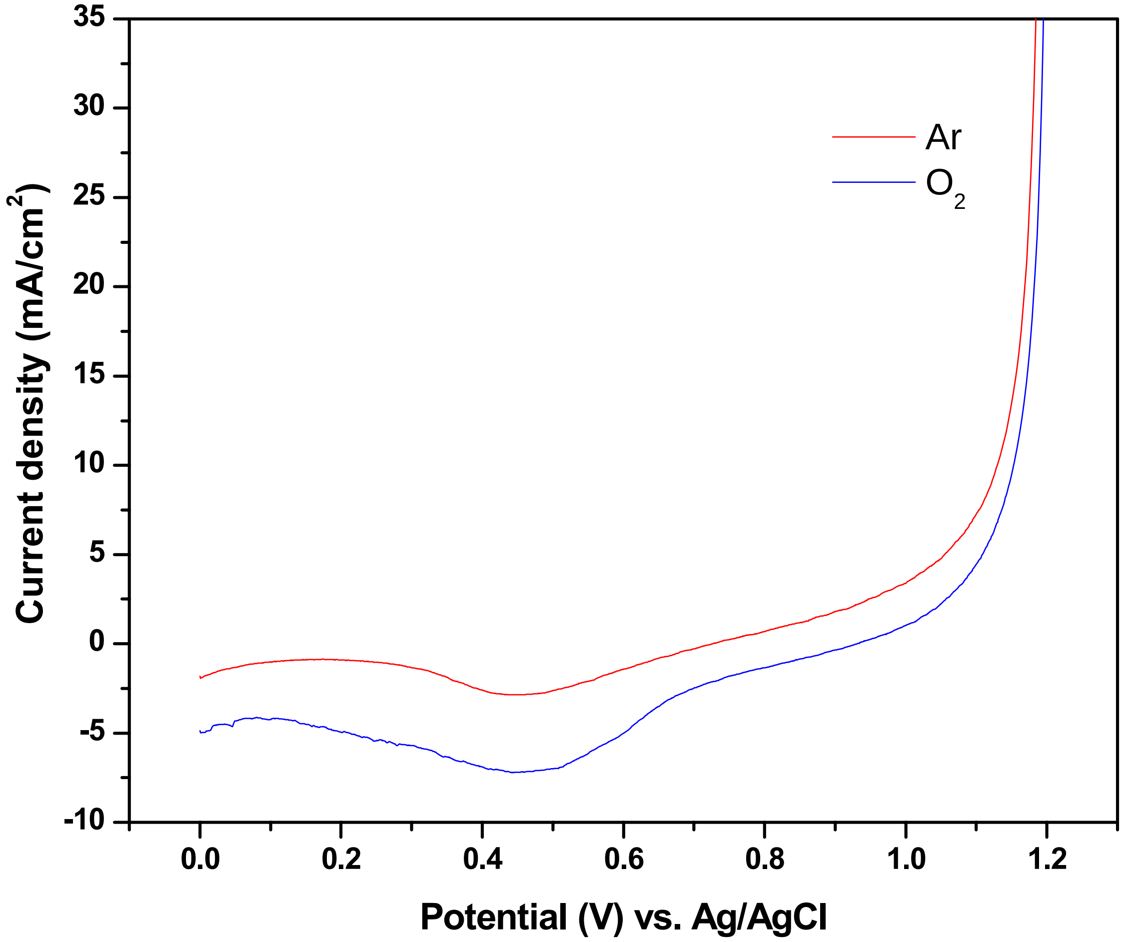

Electrolyte : 0.5M H_2SO_4; Scan rate: 5mV /s

ORR activity for Pt/C by linear sweep voltammetry

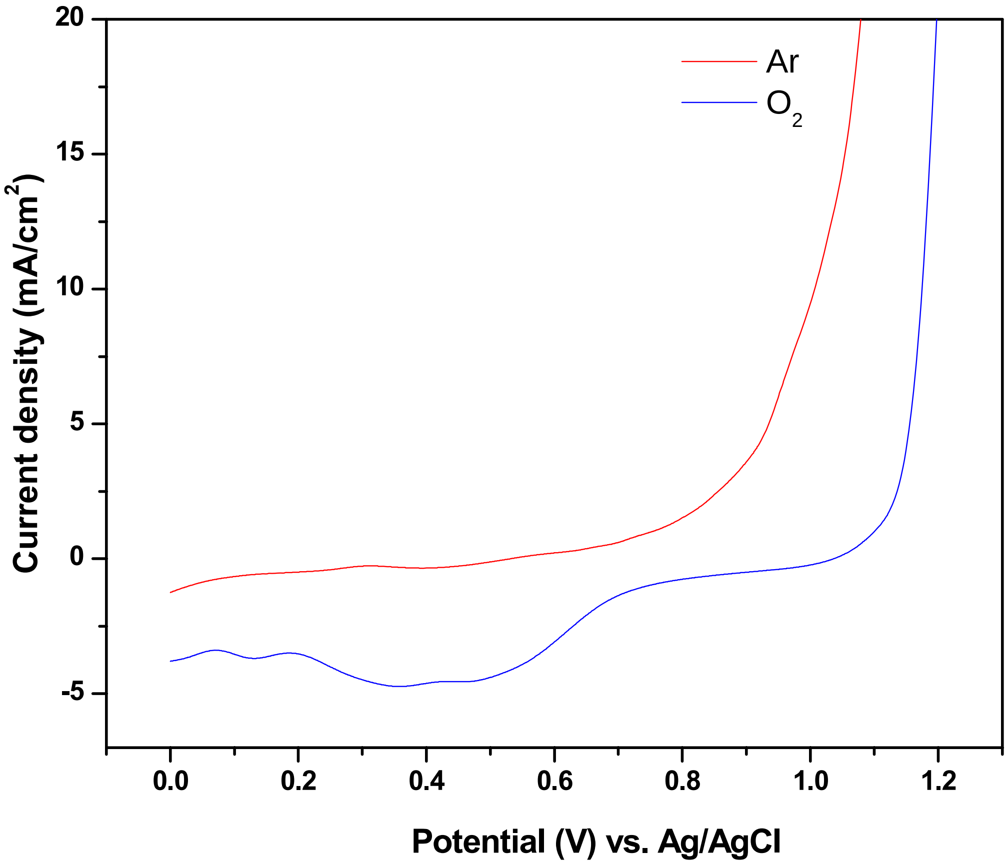

Electrolyte : 0.5M H_2SO_4; Scan rate: 5mV /s

Comparison of ORR activity for STA free and STA containing Pt/C

S.No	Current density at 0.7V in O_2 atmosphere (mA/cm^2)	Current density at 0.7V in Ar atmosphere (mA/cm^2)	Electrocatalytic activity at 0.7V (mA/cm^2)
20%Pt/STA-C	2.47	0.27	2.20
20%Pt/C	1.36	0.60	0.76

Efficient H_2O_2 reduction on Pt/STA-C

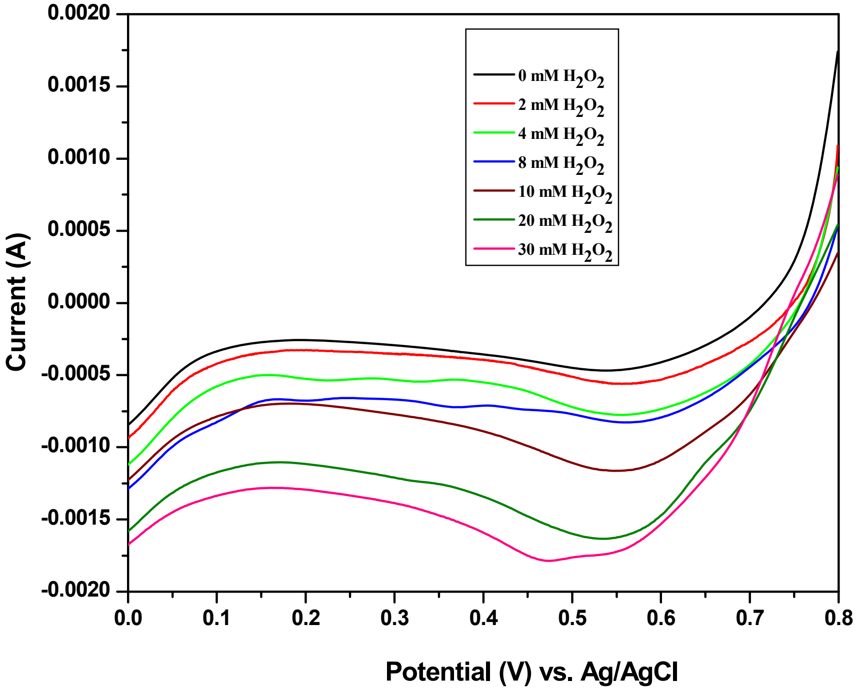

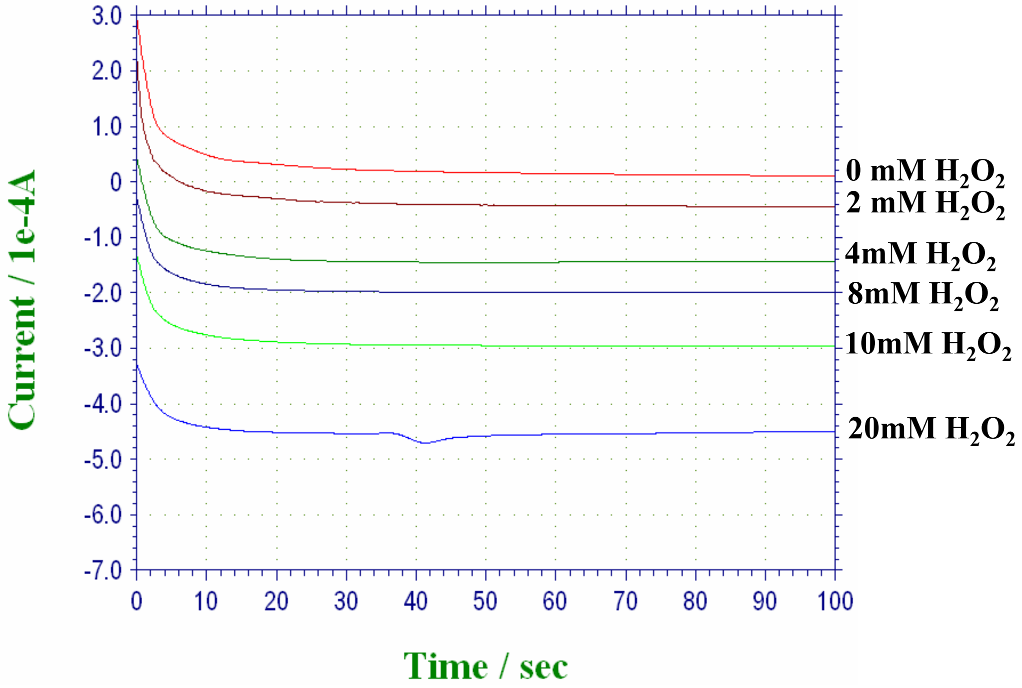

Electrolyte : 0.5M H_2SO_4; Scan rate: 25mV /s

- STA modified electrodes have improved the electrocatalytic activity of Pt nanoparticles

- The excellent reduction ability of STA containing electrodes towards H_2O_2 could be the primary reason for high catalytic activity

Conclusions

Synthesis of metal nanoparticles using POMs as Photocatalysts and stabilizers

Efficient e- transfer from POM to metal ions

$$\mathrm{POM} + \mathrm{S} \rightarrow \mathrm{POM(e^-)} + \mathrm{S_{ox}} \qquad (1)$$

$$\mathrm{POM(e^-)} + \mathrm{M^{n+}} \rightarrow \mathrm{POM} + \mathrm{M^0_{coll}} \qquad (2)$$

$$2[\mathrm{SiW_{12}O_{40}}]^{4-} + \mathrm{(CH_3)_2CHOH} \xrightarrow{h\nu} 2[\mathrm{SiW_{12}O_{40}}]^{5-} + \mathrm{(CH_3)_2C{=}O} + 2\mathrm{H^+} \qquad (3)$$

$$n[\mathrm{SiW_{12}O_{40}}]^{5-} + \mathrm{M^{n+}} \rightarrow n[\mathrm{SiW_{12}O_{40}}]^{4-} + \mathrm{M^0} \qquad (4)$$

S = propan-2-ol

$\lambda > 320$nm

$M^{n+} = Ag^+, Pd^{2+}, Au^{3+}$, and Pt^{4+}

$[SiW_{12}O_{40}]^{4-}/[SiW_{12}O_{40}]^{5-}$ (0.057 V vs. NHE)

Ag^+/Ag^0 (0.799 V vs. NHE)

$AuCl_4^-/Au^0$ (0.99 V vs. NHE)

Pd^{2+}/Pd^0 (0.987 V vs. NHE)

$PtCl_6^{2-}/Pt^0$ (0.725 V vs. NHE)

Characteristic absorption of the one-electron reduced, blue POM, $[SiW_{12}O_{40}]^{5-}$ at 730 nm

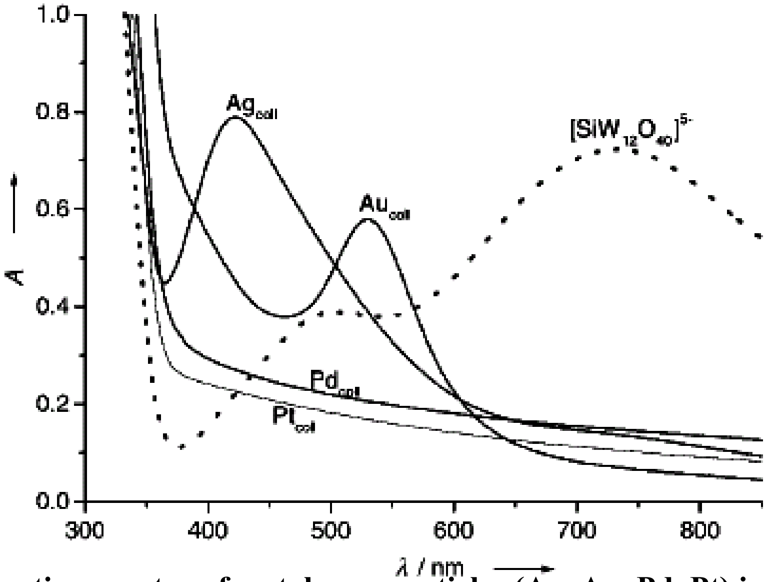

Absorption spectra of metal nanoparticles (Ag, Au, Pd, Pt) in solution

Angew. Chem. Int. Ed. 2002, 41(11), 1911

Diameter of keggin type POM = 1.2 nm can be considered spherical

Transition metal substitution in addenda atom

$PTW_{11}O_{40}^{n-}$	E (V) Vs. Ag/AgCl
$PW_{12}O_{40}^{3-}$	-0.035
$PFe(III)W_{11}O_{40}^{6-}$	+0.039
$PV(V)W_{11}O_{40}^{4-}$	+0.394
$PMn(III)W_{11}O_{40}^{4-}$	+0.924
$PCr(III)W_{11}O_{40}^{4-}$	+1.064

$PTMo_{11}O_{40}^{n-}$	E (V) Vs. Ag/AgCl
$PMo_{12}O_{40}^{3-}$	0.340
$PVMo_{11}O_{40}^{4-}$	0.510
$PV_2Mo_{10}O_{40}^{5-}$	0.480
$PV_3Mo_9O_{40}^{6-}$	0.476

Standard redox potential vs. NHE

Cr^{3+}/Cr^{2+} = -0.407 V W^{6+}/W^{5+} = -0.029 V

Fe^{3+}/Fe^{2+} = +0.771V Mo^{6+}/Mo^{5+} = 0.482 V

V^{5+}/V^{4+} = +1.00 V Mn^{3+}/Mn^{2+} = 1.541 V

I. A. Weinstock, *Chem. Rev.*, **98** (1998) 113.
Athilakshmi and B. Viswanathan, *Indian. J. Chem. B*, **37** (1998) 1186.

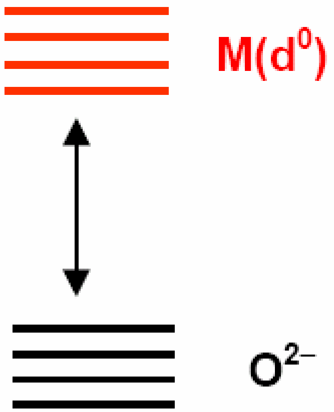

HOMO-LUMO gap (eV)

PW_{12}	SiW_{12}	AlW_{12}
2.80	2.84	2.81
PMo_{12}	$SiMo_{12}$	$AlMo_{12}$
2.03	2.06	2.04

LUMO

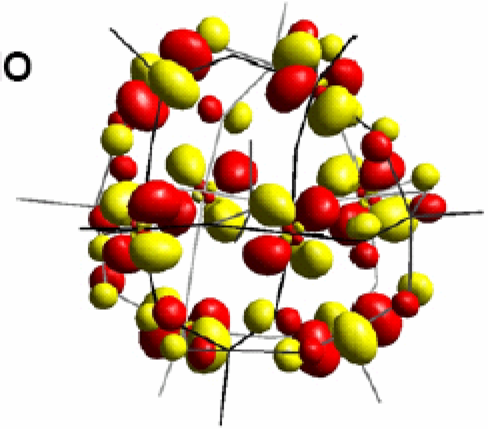

HOMO